The role played by carbonate cementation in controlling reservoir quality of the Triassic Skagerrak Formation, Norway

Yufeng Cui[a, b], Stuart J. Jones[b], Christopher Saville[b], Stephan Stricker[b], Guiwen Wang[a], Longxun Tang[b], Xuqiang Fan[a], Jing Chen[a]

[a] State Key Laboratory of Petroleum Resources and Prospecting, China University of Petroleum, Beijing 102249, China

[b] Department of Earth Sciences, Durham University, South Road, Durham, DH1 3LE, UK

Abstract

Anomalously high porosities up to 30% at burial depth of >3000 m along with varying amounts and types of carbonate cements occur in the fluvial channel sandstone facies of the Triassic Skagerrak Formation, Central Graben, Norway. However, porosities of the Skagerrak Formation are lower in the Norwegian sector than in the UK sector. In this study, petrographic analysis, core examination, scanning electron microscopy, elemental mapping, carbon and oxygen isotope, fluid inclusion and microgeometry analysis are performed to determine the diagenesis and direct influence on reservoir quality, with particular focus on the role played by carbonate cementation. The sandstones are mainly fine-grained lithic-arkosic to sub-arkosic arenites and display a wide range of intergranular volumes (2.3% to 43.7% with an average of 23.6%). Porosity loss is mainly due to compaction (av. 26.6%) with minor contribution from cementation (av. 12.1%). The carbonate cements are patchy in distribution (from trace to 20.7%) and appear as various types e.g. calcretes (i.e. calcareous concreted gravels), poikilitic sparite and sparry ferroan dolomite, and euhedral or/and aggregated ankerite/ferroan dolomite crystals. This study highlights the association of carbonate precipitation, with the remobilisation of carbonate from intra-Skagerrak calcretes during early burial stage i.e. <500 m. During deeper burial, compaction is inhibited by carbonate cements, resulting high intergranular volume of up to 32% and 29% for fine- and medium-grained sandstones, respectively. Carbonate cement dissolution probably results from both meteoric water flow with CO_2 during shallow burial, and organic CO_2 and carboxylic acid during deep burial. The maximum intergranular volume enhanced by dissolution of early carbonate cements is calculated to 8% and 5% for fine- and medium-grained sandstones, respectively. Compaction continues to exert influence after dissolution of carbonate cements, which results in a loss of ~6 % intergranular volume for fine- and medium-grained sandstones. Reservoir quality of the Norwegian sector is poorer than that of

the UK sector due to a lower coverage of clay mineral coats e.g. chlorite, later and deeper onset of pore fluid overpressure, lower solubility of carbonate compared to halite, and a higher matrix content.

Key words: carbonate cementation; dissolution; secondary porosity; reservoir quality; Skagerrak Formation; Norwegian sector

1. Introduction

Carbonate cements are a common authigenic mineral in many sandstones, and thus an understanding of the role played by carbonate is vital for reservoir evaluation. They have been the subject of research for decades mainly focusing on formation mechanisms (e.g. Asquith, 1979; Chowdhury and Noble, 1996; Dutton and Flanders, 2004; Irwin et al., 1977; Purvis and Wright, 1991; Salomons et al., 1978) and more recently effects on reservoir quality (e.g. Dutton, 2008; Taylor, 1990; Wang et al., 2016; Xiong et al., 2016). Early-precipitation of pore-filling carbonates could increase the pressure-resistance of reservoir sandstones and provide a chance for subsequent dissolution (Chi et al., 2003; Morad et al., 2010), whereas late-precipitation of carbonate cements filling residual pores could reduce the final porosity. Therefore, the timing of precipitation, dissolution and distribution of carbonate cements exert significant effect on reservoir quality.

Carbonate cements occur with various types and a wide range of content in the Skagerrak Formation in the Central Graben (UK and Norwegian sectors) along with exceptional porosities up to 30% at burial depth of >3000 m. It merits attention that porosities are significantly higher in the UK sector than in the Norwegian sector. Previous studies attribute the exceptional reservoir porosities to chlorite coats (Stricker et al., 2016a; Stricker et al., 2016b; Taylor et al., 2015), overpressure (Grant et al., 2014; Nguyen et al., 2013; Stricker et al., 2016a; Stricker et al., 2016b), halite dissolution (Nguyen et al., 2013) and limiting time for quartz cement due to rapid burial (Maast, 2016). However, the occurrence of various carbonate cements within fluvial channel facies has been neglected.

This paper aims to highlight the role that carbonate cements play in reservoir quality of the Triassic Skagerrak Formation in the Norwegian sector. A multidisciplinary approach has been undertaken to identify why anomalously high porosities occur in the Norwegian sector

but they are still lower than porosities from the same fluvial sandstone reservoirs in the UK sector.

2. Geological setting

The Central Graben of the North Sea is approximately 550 km long with a width of 70-130 km. The Central Graben is the southern arm in an incipient ridge-ridge triple junction in the North Sea, with the Viking Graben as the northern arm and the Moray Firth Basin as the western arm. The Central Graben is divided into the East and West Central Graben by Josephine High and Forties-Montrose High and separates the Norway continental shelf from United Kingdom continental shelf (Fig. 1). At least two major rifting phases in the complex rift system, one in the Permian-Triassic (290-210 Ma) and a second in the Late Jurassic (155-140 Ma), have influenced the evolution of Central Graben (Glennie, 2009; Gowers and Sæbøe, 1985). The geological history of Central Graben has been commonly divided into prerifting, synrifting, and postrifting phases (Clark et al., 1999). Synrifting sediments are dominated by siliciclastic Triassic and Jurassic sediments up to 2000 m in thickness. The postrifting sediments from the Cretaceous to the Holocene are mainly siliciclastic rocks of approximately 4500 m in thickness. The siliciclastic postrifting sediments are dominated by shale, sandstone, silty sandstone, and a thick chalk succession (Goldsmith et al., 2003). This study focuses on the East Central Graben on the Norway continental shelf, including samples from the Cod field (well 7/11-7R), Ula field (well 7/12-6), Gaupe field (well 6/3-1) as well as other 8 further wells (Fig. 1). The sandstones of the Skagerrak Formation in the Norwegian East Central Graben commonly have a patchy distribution of carbonate cements and provide a good opportunity to study the role of carbonate cements in reservoir quality.

Skagerrak stratigraphy

The Triassic strata of the Central North Sea area were deposited in a closed or internally draining basin with no marine influence (Goldsmith et al., 2003). The stratigraphy of the Triassic in the area of Central Graben was defined by Goldsmith et al. (1995) and Nedkvitne et al. (1993) on the basis of biostratigraphic and lithostratigraphic studies, along with well log correlation. The Triassic strata are generally divided into the Early Triassic mud-prone Smith Bank Formation and the Middle to Late Triassic overlying sand-prone Skagerrak Formation (Fig. 2). The Skagerrak Formation contains deposits of 500 m to 1000 m of mainly continental braided and meandering fluvial systems and terminal fluvial fans with lacustrine facies (De Jong et al., 2006; McKie, 2014). The Skagerrak Formation in the UK sector is divided into three sand-prone members (i.e. Judy, Joanne and Josephine) and three mud-prone members (i.e. Julius, Jonathan and Joshua) (Goldsmith et al., 2003; McKie and Audretsch, 2005), but these subdivisions are difficult to identify in the Norwegian sector (Fig. 2) (McKie, 2014). The sand-prone units comprise a mosaic of stacked braided fluvial channels, whereas the mud-prone units contain non-reservoir floodplain, playa and lacustrine sediments (Goldsmith et al., 1995; McKie, 2014). The Skagerrak Formation succession of alternating sand-prone and mud-prone members is the product of climatic fluctuation within the headwater of the fluvial drainage (McKie, 2014). Because of erosion during the Middle and Late Jurassic, the preservation of Triassic stratigraphy is incomplete (Fig. 2) (Erratt et al., 1999).

The Triassic sediments accumulated in a series of salt walled mini-basins, or pods, within the overall rift controlled basin (Matthews et al., 2007; Smith et al., 1993). The thick Permian Zechstein salt in the Late Permian exerted a significant control on sedimentation in the Late Permian by forming salt withdrawal minibasins as a result of a combination of salt dissolution, sediment loading, regional evacuation and structural extension (e.g. Bishop, 1996; Matthews et al., 2007; McKie, 2014; Smith et al., 1993). The Smith Bank Formation,

representing the basal part of the pod fills, was deposited in lacustrine and playa settings (Stricker et al., 2016a). The Smith Bank Formation shows highly variable thicknesses and mini-basin geometries, i.e. a tortuous basin floor topography, which probably records sediment loading and dissolution in the course of initial fluvial sediment supply into the desiccated Zechstein basin (Fig. 3) (McKie, 2014; McKie and Audretsch, 2005). The subsequent deposition of the Skagerrak Formation in the study area occurred within interpod palaeovalleys and fed Late Triassic fluvial systems and terminal fans (Fig. 3) (Stewart and Clark, 1999), and was not significantly confined or guided by the underlying salt on a basin scale (McKie, 2014).

3. Methodology

3.1 Sampling

Core samples and thin sections examined in this study are from Middle to Late Triassic Skagerrak Formation of three Norwegian fields: the Cod field (7/11-7R, 32 samples), the Ula field (7/12-6, 26 samples), and the Gaupe field (6/3-1, 81 samples). Furthermore, 32 samples, from 2/5-10, 2/8-12, 7/7-1, 7/7-2, 7/11-6, 7/11-8, 7/11-10S and 7/11-12S wells have been also selected for analsysis. The depth of the 171 samples used in this study ranges from 3025 m to 5342 m.

3.2 Petrography

A total of 237 thin sections were analysed from core samples. Thin section scanning images were obtained using Dimage Scan Elite II. Based on these images optical porosity, grain size and pore size were measured using digital image analysis technique jPOR (Grove and Jerram, 2011) and ImageJ software (1.51f) (Ferreira and Rasband, 2012). 132 thin sections were analysed by point counting with 300 counts per thin section. A further 31 thin sections were

selected based on the content of carbonate cements (higher than 5% by point counting) and stained with Alizarin Red S and potassium ferricyanide to identify carbonate cement types. Highly polished thin sections without coverslips and 44 core rock samples were coated with carbon prior to examination with a Hitachi TM 1000 scanning electron microscopy (SEM) equipped with an energy-dispersive spectroscopy (EDS). Elemental mapping was also undertaken using the SEM on the above 9 thin sections to determine the minerals and their distribution. Helium porosity of 839 core samples has been examined in core samples from all wells in this study. To determine the source of the carbonate cement, four samples with high volume of calcite cement were selected and stable isotope ratios of carbon and oxygen were analysed by CO_2 liberation method. Stable carbon and oxygen isotope data were presented in the δ notation relative to Vienna Pee Dee Belemnite (VPDB) standard. In addition, 85 fluid inclusions from six samples were examined.

4. Results

4.1 Grain composition and texture

The sandstones of the Skagerrak Formation comprise monocrystalline quartz (34.7% to 91.9% averaged at 62.2% among framework grains), feldspar (4.0% to 52.9% averaged at 26.2% among framework grains) including both K-feldspar and plagioclase, and metamorphic and argillaceous sedimentary rock fragments (<1.0% to 37.6% among framework grains). According to Folk's classification (Folk, 1974), the sandstones are mainly fine-gained lithic-arkosic to arkosic sandstones (Fig. 4). Grains are moderately to well sorted and sub-angular to sub-rounded. Grain size (analysed arithmetic mean value for each thin section using ImageJ) varies from 69.5 μm to 427.0 μm averaged at 160.8 μm (Fig. 5; see the supplementary material for the data).

4.2 Porosity and pore size distribution

Helium porosities of the Skagerrak Formation samples range from 1.3% to 25.9% and mainly occur between 10% and 20% with an average of 12.7% (Fig. 6), whereas the optical porosities analysed using thin section show a wider range (from 0.01% to 30%) and a lower average of 8.4%. Pores are mainly intergranular pores, including primary and secondary pores, and minor amounts of intragranular pores after dissolved feldspars. The pore size (analysed arithmetic mean value for each thin section using ImageJ) in Skagerrak sandstones varies from 47.9 μm to 123.7 μm with an average of 76.6 μm (Fig. 7A and B, see the supplementary material for the data). The pore area (the corresponding area of each pore size) ranges from 629 μm^2 to 7792 μm^2 averaged at 2288 μm^2 (Fig. 7C and D; see the supplementary material for the data). With respect to the pore size distribution, most of the silt-grained samples show a single peak around 90 μm, whereas the fine- and medium-grained samples tend to have a similar main peak with additional sub-peaks with values greater than 90 μm (Fig. 7C and D), i.e. fine- and medium-grained samples have much larger pore size than silt-grained samples.

4.3 Intergranular volume and porosity loss

Intergranular volume (IGV) is the sum of intergranular pore space, intergranular cement, and depositional matrix (Houseknecht, 1987; Paxton et al., 2002). In a historical view, IGV is very similar to the concept of "minus-cement porosity" which, however, does not include matrix (Paxton et al., 2002). In combination with the measured total cement volume (C) and initial porosity (P_i) , the IGV can be used to calculate compactional porosity loss (COPL), and cementational porosity loss (CEPL) using the following equations (Lundegard, 1992):

$$COPL = P_i - \left(\frac{(100 - P_i)P_{mc}}{100 - P_{mc}} \right) \quad (1)$$

$$CEPL = (P_i - COPL)(\frac{C}{P_{mc}}) \quad (2)$$

Where P_i is the initial porosity (assumed 45%; Beard and Weyl, 1973; Lundegard, 1992), and P_{mc} is intergranular volume (IGV). If two conditions, including correct assumed initial porosity P_i, negligible internally derived cement and grain dissolution, are met, the calculated COPL and CEPL are accurate (Lundegard, 1992). In this study, the initial porosity in Skagerrak Formation sandstones is assumed to be 45% (Lundegard, 1992; Paxton et al., 2002; Stricker et al., 2016a). The plot of COPL vs. CEPL shows that porosity loss is mainly due to compaction (av. 26.6%) and less due to cementation (av. 12.1%) (Fig. 8A). Intergranular volume (IGV) values have a wide range from 2.3% to 43.7% with an average of 23.6%. In addition, IGV values show positive relationship with matrix content (Fig. 8B), which ranges from trace to 35.5% with an average of 11.7%. The matrix is mainly depositional clay matrix (Taylor et al., 2015).

4.4 Diagenetic minerals

4.4.1 Quartz cements

Quartz cementation in the Skagerrak Formation occurs as three types including syntaxial overgrowths, euhedral quartz crystals and microquartz (Fig. 9A-C). Syntaxial quartz overgrowths show generally greater thicknesses ranging from 20 μm to 150 μm, with some overgrowths partly replaced by carbonate cements (Fig. 9A). Euhedral quartz crystals are smaller compared to syntaxial overgrowths with crystal sizes <60 μm and show a patchy distribution and prismatic outgrowths which engulf clay coatings (Fig. 9B). Microquartz only occurs as grain coatings with crystal sizes <10 μm (Fig. 9C) (Vagle et al., 1994), and shows a parallel to sub-parallel c-axes orientation to the host grain surface (Fig. 9C) (French and

Worden, 2013). Macroquartz overgrowths are not observed when microquartz is present (Fig. 9C).

4.4.2 Clay minerals

Clay minerals in Skagerrak Formation are authigenic and include chlorite, illite and smectite. These clay minerals appear with varied amounts and types. Chlorite is the most common authigenic clay mineral, ranging from trace to 12.3% with an average of 2.5%. Chlorite occurs as small flakes (about 4 μm) which coat the grains (Fig. 9D) and are engulfed by euhedral quartz crystals (Fig. 9B). Chlorite coats in the Skagerrak Formation are intermediate according to the Fe/Mg-ratio (Stricker et al., 2016b), and show a wide grain coverage range from 1.3% to completely grain coating (100%) with an average of 48.0%. The thickness of the chlorite coats is generally less than 15 μm. Illite, ranging from trace to 4.0% with an average of 1.49%, is observed as hair-like filamentous pore lining (Fig. 9E). Smectite ranges from trace to 6.80% (av. 1.67%) and usually occur as smooth grain coatings and also as pore bridges between adjacent grains (Fig. 9F). The coexistence of illite and chlorite is rarely observed.

4.4.3 Carbonate cements

Carbonate cements show a patchy distribution (trace to 20.7%) in the Skagerrak Formation and have a wide variety of types, including calcretes (i.e. calcareous concreted gravels; Lamplugh, 1902), poikilitic sparite, sparry ferroan dolomite, and euhedral or/and aggregated ankerite/ferroan dolomite crystals (Fig. 10; Fig. 11A and B). Calcretes are spherical to oval shaped and vary in diameter from a few tens of microns up to around 5 cm (Fig. 10A-C). Calcretes are common in poorly sorted sandstones. Neighbouring grains of calcretes tend to be extensively cemented (Fig 10B, C). The occurrence of poikilitic sparite and sparry ferroan dolomite is common in the moderately to well sorted, sub-rounded to

rounded and fine- to medium-grained sandstones, filling prevalently intergranular pores (Fig. 10D and E; Fig. 11A). Partial replacement of framework grains by carbonate cements is also found in sparry cemented sandstones and the rims of the etched grains are embayment shaped (Fig. 10D and E). Euhedral or/and aggregated ankerite/ferroan dolomite crystals show a patchy occurrence (Fig 10G-I) and are frequently associated with highly porous sandstones (Fig. 10G; Fig. 11A). Dissolution of carbonate cements also occurs on the rims of the cements (Fig. 10I). The limited carbon and oxygen isotope data for carbonate cements show a narrow range of $\delta^{18}O$ values (-5.39‰ to -2.76‰ in VPDB) but a wide range of $\delta^{13}C$ values (-9.99‰ to 2.04‰ in VPDB) (Fig. 12).

4.4.4 Other minerals

Abundant halite has been reported by Nguyen et al. (2013) in Skagerrak Formation sandstones in the J-Block, UK sector. However, much less halite (from trace to 4.0%, av. 0.51%) occurs as a patchy distribution in the Norwegian sector. Other diagenetic minerals such as pyrite and K-feldspar overgrowths occur in negligible amounts (Stricker et al., 2016b; Taylor et al., 2015).

4.5 Dissolution

Mineral dissolution is an important process in the Skagerrak Formation sandstones and mainly occurs in feldspars and carbonate cements. Partial to nearly complete dissolved feldspars are observed with micro to macro pores (Fig. 13A-C). Feldspar dissolution occurs along cleavages and rims showing the morphology of honeycomb or fence (Fig. 13A and B). The secondary porosity formed from feldspar dissolution is minor ($\leqslant$1%). Although it is hard to quantify the carbonate cement dissolution, numerous evidences show the existence of carbonate dissolution. Remnants of carbonate cements show embayment shaped rims

indicating the occurrence of carbonate dissolution (Fig. 10I). Though, in some cases, no cement remnant is found, embayment shaped rims of framework grains also suggest early replacement and subsequent dissolution (see discussion). The sandstones samples with anomalously high porosity regarding to normal porosity trends (e.g. Ramm and Bjørlykke, 1994; Sclater and Christie, 1980) are likely to have grains with irregular embayment shaped rims (Fig. 13D), which appear to be morphologically similar to the grain surfaces seen in thin section of sandstones with carbonate cements (Fig. 10D; Fig. 11A).

5. Discussion

5.1 Paragenetic sequence

A diagenetic sequence (Fig. 14) of the Skagerrak Formation sandstones is primarily based on petrographic features (Figs. 9-11, 13 and 15). Burial history model (well 7/11-7R) shows that the Skagerrak Formation in the Norwegian sector experienced an early shallow burial phase over a long period of time, and then went rapidly into deep burial phase until present day (Stricker et al., 2016a). Macroquartz cementation starts generally at temperature between 70 °C and 80 °C (McBride, 1989; Walderhaug, 1994; Walderhaug, 1996). Authigenic clay coatings and microquartz overgrowths inhibiting macroquartz should predate macroquartz cementation (Fig. 9C, D and F). Replacement of quartz overgrowths by carbonate cements is observed (Fig. 9A; Fig. 10D), indicating that alteration and reprecipitation of carbonate cements postdates macroquartz cementation. In addition, according to the isotopic analysis, there should be an early episode of calcite cementation (discussed in section 5.4.2). Traces of halite were found associated with calcite in the same pore spaces, which suggests that sources for these cements in the UK sector and Norwegian sector are related, and they precipitated at the similar time. Secondary pores from dissolved and corroded feldspars are not cemented by calcite cement but partly by ankerite/ferroan dolomite (Fig. 13C), which indicates that the

dissolution of feldspars predates ankerite/ferroan dolomite cement and postdates calcite cement. Dissolution of calcite and halite occurs over a wide burial depth range due to meteoric water leaching, and organic CO_2 and carboxylic acid etching (discussed in section 5.4.3). The ankerite/ferroan dolomite cement also shows evidence of dissolution. Little ferroan calcite is found and assumed to precipitate and dissolve at the same time as ankerite/ferroan dolomite. Based on the homogenization temperature of the hydrocarbon fluid inclusion (Fig. 15), the temperature during hydrocarbon filling is around 75-100 °C.

5.2 Porosity-depth trends in Skagerrak Formation

Porosity-depth trends of North Sea sediments have been the subject of previous studies, e.g. Sclater and Christie (1980) proposing an exponential relation for porosity-depth trends for normal pressured lithologies, or Ramm and Bjørlykke (1994) using a linear regression for porosity prediction (Fig. 16). Porosities in the Norwegian sector have a wide range and show anomalously high values (up to about 30% at the burial depth of >3000 m) consistent with Ramm et al. (1997). However, porosities are lower in the Norwegian sector than in the UK sector (Fig. 16; the reason will be discussed in section 5.3). Ramm et al. (1997) attributed anomalously high porosity to ubiquitous microquartz coatings in the Upper Jurassic reservoirs in the Norwegian Central Graben. Grant et al. (2014) and Stricker et al. (2016b) considered shallow onset of overpressure as an important control on the exceptional porosity in the Skagerrak Formations in the UK sector. In addition to overpressure, Nguyen et al. (2013) also ascribed the anomalously high porosities in the Skagerrak Formation to the late dissolution of grain framework stabilising halite. However, based on this petrographic study and previous research, there is no evidence for the pervasive occurrence of microquartz and halite in the sandstones of the Skagerrak Formation. Overpressure was generated during late and deep burial history in the Skagerrak Formation in the Norwegian sector. High pore fluid

pressure (low vertical effective stress) and rate of overpressure development played a minor role in maintaining reservoir quality.

5.3 Comparison with Skagerrak Formation in UK sector

The reservoir quality decrease from the UK to Norwegian sectors (Fig. 16) is most likely attributed to a combination of factors including chlorite coats, overpressure, cement types, and matrix content. Chlorite has been widely reported as an important grain coating clay mineral inhibiting quartz overgrowth and help preserve porosity (Bloch et al., 2002; Ehrenberg, 1993; Stricker and Jones, 2016; Taylor et al., 2010). Bloch et al. (2002) and Ajdukiewicz and Lander (2010) reported the significance of the coat continuity (or grain surface coverage) on the prevention of quartz cementation. The surface coverage of chlorite coats in the Norwegian and UK sector are 48% and 80% in average, respectively (Stricker et al., 2016b). Therefore, one explanation for the reduced porosity in the Norwegian sector is the lower chlorite coverage. Nguyen et al. (2013), Grant et al. (2014) and Stricker et al. (2016a) illustrated the significant effect of overpressure and vertical effective stress reduction for porosity preservation in the UK sector. Overpressure in the Norwegian sector started to develop later (reaching 1 MPa at 35 Ma), and deeper (reaching 1 MPa at about 2250 m) (Stricker et al., 2016a). Hence overpressure and importantly low vertical effective stress has less impact upon porosity maintenance in the Norwegian sector, which explains the poorer reservoir quality and higher degree of compaction. Nguyen et al. (2013) documented the significant effect of halite dissolution on reservoir quality in the UK sector, whereas porosity enhancement in the Norwegian sector is due to carbonate dissolution (discussed in section 5.4.1). As carbonate has much lower solubility than halite, the occurrence of different cement types (i.e. halite and carbonate) is another explanation for lower porosity in the Norwegian sector. Moreover, the matrix content is higher in the Norwegian sector (av. 11.7%; Fig. 8)

than in the UK sector (av. 1.2%; Taylor et al., 2015), which also accounts for the reduced reservoir quality.

5.4 Carbonate cements

5.4.1 Role in reservoir quality

Three criteria for identification of secondary porosity after the dissolution of carbonate cements in sandstones have been proposed by Schmidt (1979). These criteria include the occurrence of oversized pores due to the dissolution of grain-replacive carbonate cements, partially dissolved carbonate cements with etched outlines, and grain-replacive carbonates surrounded by open pores. Burley and Kantorowicz (1986) also presented several textual criteria such as corroded grain margins for recognition of cement dissolution from thin section and SEM. Most of these criteria of carbonate cement dissolution can be observed in Skagerrak Formation, especially the etched outlines both in framework grains and carbonate cements (Fig. 10; Fig. 13). Carbonate cements demonstrate a positive correlation with porosity at low carbonate cements content (<~9%), whereas porosity decreases dramatically with carbonate cements increasing at high carbonate cements content (>~9%) (Fig. 17), which relates to varying intensity of carbonate cementation and dissolution. Unlike the dissolution of feldspars, the pores from carbonate cement dissolution are generally difficult to be distinguished from primary pores (i.e. pores without cements during burial history). Thus precise determination of secondary porosity from the dissolution of carbonate cements is difficult to achieve. However, if the following three conditions are met, the intergranular volume preserved by early carbonate cements could be determined. First, carbonate cements in tightly cemented sandstones are the early carbonate cements. Second, the anomalously high porosity is caused by dissolution of early carbonate cements. Third, tightly compacted and/or quartz cemented sandstones represents sandstones without or with negligible

carbonate cement precipitation and dissolution during burial history. Based on the intergranular volume (IGV) and intergranular pore size determined using petrographic analysis, there are differences between the IGV values in tightly cemented sandstones and uncemented sandstones (with anomalously high porosity), and between the IGV values of uncemented sandstones and tight sandstones (i.e. tightly compacted and/or quartz cemented sandstones) (Fig. 18). According to these differences, the conclusion can be drawn that compaction continues to contribute to porosity loss of ~6% for fine- and medium-grained sandstones after carbonate dissolution. IGV preserved by carbonate cements (i.e. combined effect of early cementation and late dissolution) is 8% and 5% for fine- and medium-grained sandstones, respectively. However, the influence of other factors such as chlorite and microcrystalline quartz cannot be completely neglected, and thus the values calculated above are maximum IGV values preserved by carbonate cements.

5.4.2 Origin of carbonate cements

Isotope data can highlight the origin of carbon and oxygen, such as plant types, the degree of isotopic equilibration with atmospheric CO_2, the mechanism of organic matter oxidation, and the precipitation temperature (Morad et al., 1998; Naylor et al., 1989; Smith and Epstein, 1971). Therefore, many controls on the isotopic composition of carbon and oxygen have been proposed in previous studies. These controls include latitude, elevation, temperature, the vegetation type and its seasonal activity, isotopic composition of the rainfall, the degree of evaporation, the distance to the sea, monsoonal influences and the degree of contamination by pre-existing carbonate in the soil (e.g. Cerling, 1984; Liu et al., 2014; Purvis and Wright, 1991; Salomons and Mook, 1986; Smith and Epstein, 1971). Because of these extremely diverse factors, a precise interpretation of the isotopic data is difficult to achieve.

Nevertheless, we use the data in this study and compare to previous studies to decipher the plausible origin of carbonate cementation.

The $\delta^{18}O$ of pore water of Triassic in Norwegian sector is referred to be about from -6‰ to -4 ‰ (av. -5‰, VSMOW; Fig. 12) (Morad et al., 1998). Based on the $\delta^{18}O$ of pore water and the fractionation equation after Friedman and O'Neil (1977), the calculated precipitation temperature of calcite cement ranges from 3 °C to 20 °C, av. 11 °C (Fig. 19), which is consistent with the result from Knox et al. (1984) and indicates precipitation of calcite cement in the shallow subsurface (i.e. <500 m). According to the calculated precipitation temperature and the petrographic characteristics that extensive carbonate cementation around the calcretes are observed (Fig. 10 A-C), it can be proposed that carbonate in the Skagerrak Formation sandstones originated from reprecipitation of intra-Skagerrak Formation calcretes. These calcretes could be sourced from reworked rhizoliths, pedogenic nodules, groundwater calcretes, and fluvial sediments (McKie, 2014; Morad, 1998). The isotopic data with lower $\delta^{13}C$ values (about -10‰, VPDB) are within the ranges of present day soil carbonates given by Salomons et al. (1978), and probably show the evaporative processes (Bath et al., 1987; Knox et al., 1984; Naylor et al., 1989), and also indicate a C4 type vegetation (Naylor et al., 1989; Salomons and Mook, 1986). However, Purvis and Wright (1991) believe that the evapo-transpiration instead of evaporation induced carbonate precipitation. But we consider that evaporative processes to dominate the carbonate precipitation because abundant calcretes occur in the study fields and calcretes generally develop in warm to hot, arid to semi-arid regions, with low seasonal rainfall and high evaporation (Goudie and Pye, 1983). Whereas, the data with higher $\delta^{13}C$ values (about 1.5‰, VPDB; Fig. 12) probably indicate carbon derivation within microbial methanogenesis zone, bacterial fermentation and contribution from atmospheric CO_2 (Irwin and Hurst, 1983; Morad et al., 1998).

5.4.3 Mechanism of carbonate cement dissolution

Dissolution of substantial amounts of pore-filling carbonate cements in sandstones is less commonly recognized and difficult to quantify, and thus the importance of dissolution of carbonate cements is debatable (Bjørlykke, 2014; Burley and Kantorowicz, 1986; Giles, 1987; Schmidt, 1979; Taylor et al., 2010). Perhaps more importantly is whether there are sufficient organic acid to dissolve the carbonate cements or significant fluid flow with undersaturated solutions to replenish the system (e.g. Taylor et al., 2010). The undersaturated pore water may be derived from formation water with carboxylic acid sourced from organic matter, meteoric water with CO_2, compactional pore water with organic CO_2, cooled deep formation water, and reactions of clay minerals (Bjørlykke, 1984; Giles and Boer, 1989; Schmidt, 1979; Surdam et al., 1984; Taylor et al., 2010). The Skagerrak Formation experienced shallow burial over a long period of time (Fig. 14), which provides a good opportunity for meteoric water with CO_2 to dissolve carbonate cements. In addition, carbon isotopic data indicate the carbon is sourced from atmospheric CO_2, suggesting that sandstones acted as an open system during shallow burial (Bjørlykke, 1984). In the Middle to Late Triassic succession, mudstones occur in episodic palustrine and marsh conditions and are rich in organic matter. Therefore, below the reach of meteoric water, i.e. during deeper burial, organic CO_2 and carboxylic acid are sourced from the organic matters and migrate into adjacent sandstones to dissolve carbonate cements (Schmidt, 1979; Surdam et al., 1984). However, no apparent faults or fractures are observed in Skagerrak Formation, and thus carbonate cements are unlikely dissolved by cooled deep formation water (Giles and Boer, 1989). Furthermore, no obvious evidence shows carbonate cement dissolution resulted from reactions of clay minerals.

6. Conclusions

1. Anomalously high porosity (up to 30% at burial depth of >3000 m) exists in the Skagerrak Formation, Norwegian sector, which is attributed to dissolution of carbonate cements in addition to high pore fluid pressures and especially chlorite grain coats referred in previous studies. Most porosity loss is due to compaction (av. 26.6%) and minor contribution is from cementation (av. 12.1%).

2. Compared with the UK sector, poorer reservoir quality is encountered in the Norwegian Skagerrak Formation due to later and deeper onset of overpressure (low vertical effective stress), lower percentage of chlorite coatings (48%), lower solubility of carbonate compared to halite, and an overall higher matrix content (up to 35.5%, av. 11.7%).

3. Carbonate cements in the Skagerrak Formation show a patchy distribution (trace to 20.7%) and a wide variety of types, including calcretes, poikilitic sparite, sparry ferroan dolomite, and euhedral or/and aggregated ankerite/ferroan dolomite crystals. At low carbonate cements content (<~9%), carbonate cementation illustrates a positive relationship with porosity.

4. The role of carbonate cementation for reservoir quality is quantified in this study. Intergranular volume preserved by carbonate cements (i.e. combined effect of early cementation and late dissolution) is 8% and 5% for fine- and medium-grained sandstones, respectively.

5. Carbonate precipitation in the Skagerrak Formation sandstones originated from calcretes sourced from reworked rhizoliths, pedogenic nodules, groundwater calcretes, and fluvial sediments. These calcretes contributing to early carbonate cements (i.e. <500 m) are indicative of a C4 type vegetation during the Triassic. Additional, later carbonate cementation is attributed to microbial methanogenesis and some contribution from atmospheric CO_2.

6. Carbonate cement dissolution is attributed to both meteoric water flow with CO_2 during shallow burial, and organic CO_2 and carboxylic acid during deep burial to maximum burial at the present-day.

Acknowledgements

The authors acknowledge support from ConocoPhillips Norge for financial support of this project and access to core and datasets. This work is also financially supported by the program of China Scholarship Council (No. 201506440024), National Natural Science Foundation of China (No. 41472115) and the National Science and Technology Major Project of China (No. 2016ZX05019005-007). The results presented have been improved through collaborative discussions with Yang Li from Durham University, Yanzhong Wang from China University of Petroleum, Qingdao, Meiyan Fu from Chengdu University of Technology, Huifei Tao from Chinese Academy of Sciences, Lanzhou, Xiang Ge from China University of Geosciences, Wuhan, and Binh T. T. Nguyen from JX Nippon Oil & Gas Exploration Corporation.

References

Ajdukiewicz, J.M., Lander, R.H., 2010. Sandstone reservoir quality prediction: The state of the art. AAPG Bulletin, 94(8): 1083-1091.

Asquith, G.B., 1979. Subsurface carbonate depositional models: a concise review. Petroleum Publishing Co.,Tulsa, OK, Medium: X; Size: Pages: 129 pp.

Bath, A., Milodowski, A., Spiro, B., 1987. Diagenesis of carbonate cements in Permo-Triassic sandstones in the Wessex and East Yorkshire-Lincolnshire Basins, UK: a stable isotope study. Geological Society, London, Special Publications, 36(1): 173-190.

Beard, D., Weyl, P., 1973. Influence of texture on porosity and permeability of unconsolidated sand. AAPG bulletin, 57(2): 349-369.

Bishop, D.J., 1996. Regional distribution and geometry of salt diapirs and supra-Zechstein Group faults in the western and central North Sea. Marine and petroleum geology, 13(4): 355-364.

Bjørlykke, K., 1984. Formation of secondary porosity: How important is it? , 59: 277-286.

Bjørlykke, K., 2014. Relationships between depositional environments, burial history and rock properties. Some principal aspects of diagenetic process in sedimentary basins. Sedimentary Geology, 301: 1-14.

Bloch, S., Lander, R.H., Bonnell, L., 2002. Anomalously high porosity and permeability in deeply buried sandstone reservoirs: Origin and predictability. AAPG bulletin, 86(2): 301-328.

Burley, S., Kantorowicz, J., 1986. Thin section and SEM textural criteria for the recognition of cement ‐ dissolution porosity in sandstones. Sedimentology, 33(4): 587-604.
Cerling, T.E., 1984. The stable isotopic composition of modern soil carbonate and its relationship to climate. Earth and Planetary science letters, 71(2): 229-240.
Chi, G., Giles, P., Williamson, M., Lavoie, D., Bertrand, R., 2003. Diagenetic history and porosity evolution of Upper Carboniferous sandstones from the Spring Valley# 1 well, Maritimes Basin, Canada–implications for reservoir development. Journal of Geochemical Exploration, 80(2): 171-191.
Chowdhury, A.H., Noble, J.P., 1996. Origin, distribution and significance of carbonate cements in the Albert Formation reservoir sandstones, New Brunswick, Canada. Marine and Petroleum Geology, 13(7): 837-846.
Clark, J., Cartwright, J., Stewart, S., 1999. Mesozoic dissolution tectonics on the west central shelf, UK Central North Sea. Marine and Petroleum Geology, 16(3): 283-300.
De Jong, M., Smith, D., Nio, S., Hardy, N., 2006. Subsurface correlation of the Triassic of the UK southern Central Graben: new look at an old problem. first break, 24(6).
Dutton, S.P., 2008. Calcite cement in Permian deep-water sandstones, Delaware Basin, west Texas: Origin, distribution, and effect on reservoir properties. AAPG bulletin, 92(6): 765-787.
Dutton, S.P., Flanders, W.A., 2004. Evidence of reservoir compartmentalization by calcite cement layers in deepwater sandstones, Bell Canyon Formation, Delaware Basin, Texas. Geological Society, London, Special Publications, 237(1): 279-282.
Ehrenberg, S., 1993. Preservation of anomalously high porosity in deeply buried sandstones by grain-coating chlorite: examples from the Norwegian continental shelf. AAPG Bulletin, 77(7): 1260-1286.
Erratt, D., Thomas, G., Wall, G., 1999. The evolution of the central North Sea Rift. In: D. Erratt, G. Thomas, G. Wall (Eds.), Geological society, london, petroleum geology conference series. Geological Society of London, pp. 63-82.
Ferreira, T., Rasband, W., 2012. ImageJ User Guide. In: T. Ferreira, W. Rasband (Eds.).
Folk, R.L., 1974. Petrology of sedimentary rocks. Hemphill Publishing Company.
French, M.W., Worden, R.H., 2013. Orientation of microcrystalline quartz in the Fontainebleau Formation, Paris Basin and why it preserves porosity. Sedimentary Geology, 284: 149-158.
Friedman, I., O'Neil, J.R., 1977. Data of geochemistry: Compilation of stable isotope fractionation factors of geochemical interest, 440. US Government Printing Office.
Giles, M.R., 1987. Mass transfer and problems of secondary porosity creation in deeply buried hydrocarbon reservoirs. Marine & Petroleum Geology, 4(3): 188-204.
Giles, M.R., Boer, R.B.D., 1989. Secondary porosity: creation of enhanced porosities in the subsurface from the dissolution of carbonate cements as a result of cooling formation waters. Marine & Petroleum Geology, 6(3): 261-269.
Glennie, K., 2009. Petroleum Geology of the North Sea: Basic concepts and recent advances. John Wiley & Sons.
Goldsmith, P. et al., 2003. The millennium atlas: Petroleum geology of the central and northern North Sea. In: P. Goldsmith et al. (Eds.), Geological Society London, pp. 105-127.
Goldsmith, P., Rich, B., Standring, J., 1995. Triassic correlation and stratigraphy in the south Central Graben, UK North Sea. Geological Society, London, Special Publications, 91(1): 123-143.
Goudie, A.S., Pye, K., 1983. Chemical sediments and geomorphology: Precipitates and residua in the near-surface environment. Academic Press Inc.(London).
Gowers, M.B., Sæbøe, A., 1985. On the structural evolution of the Central Trough in the Norwegian and Danish sectors of the North Sea. Marine and Petroleum Geology, 2(4): 298-318.
Grant, N.T., Middleton, A.J., Archer, S., 2014. Porosity trends in the Skagerrak Formation, Central Graben, United Kingdom Continental Shelf: The role of compaction and pore pressure history. AAPG bulletin, 98(6): 1111-1143.

Grove, C., Jerram, D.A., 2011. jPOR: An ImageJ macro to quantify total optical porosity from blue-stained thin sections. Computers & Geosciences, 37(11): 1850-1859.
Houseknecht, D.W., 1987. Assessing the relative importance of compaction processes and cementation to reduction of porosity in sandstones. AAPG bulletin, 71(6): 633-642.
Irwin, H., Curtis, C., Coleman, M., 1977. Isotopic evidence for source of diagenetic carbonates formed during burial of organic-rich sediments.
Irwin, H., Hurst, A., 1983. Applications of geochemistry to sandstone reservoir studies. Geological Society, London, Special Publications, 12(1): 127-146.
Knox, R.B., Burgess, W., Wilson, K., Bath, A., 1984. Diagenetic influences on reservoir properties of the Sherwood Sandstone (Triassic) in the Marchwood geothermal borehole, Southampton, UK.
Lamplugh, G.W., 1902. 'Calcrete.'. Geological Magazine, 9: 575-575.
Liu, S., Huang, S., Shen, Z., Lü, Z., Song, R., 2014. Diagenetic fluid evolution and water-rock interaction model of carbonate cements in sandstone: An example from the reservoir sandstone of the Fourth Member of the Xujiahe Formation of the Xiaoquan-Fenggu area, Sichuan Province, China. Science China Earth Sciences, 57(5): 1077-1092.
Lundegard, P., 1992. Sandstone porosity loss. A ''big picture''view of the importance of Compactation. Journal of Sedimentary Research, 62: 250-260.
Maast, T.E., 2016. Overpressure preventing quartz cementation?–Comment to Stricker et al.(2016). Marine and Petroleum Geology.
Matthews, W.J., Hampson, G.J., Trudgill, B.D., Underhill, J.R., 2007. Controls on fluviolacustrine reservoir distribution and architecture in passive salt-diapir provinces: Insights from outcrop analogs. AAPG bulletin, 91(10): 1367-1403.
McBride, E.F., 1989. Quartz cement in sandstones: a review. Earth-Science Reviews, 26(1): 69-112.
McKie, T., 2014. Climatic and tectonic controls on Triassic dryland terminal fluvial system architecture, central North Sea. From Depositional Systems to Sedimentary Successions on the Norwegian Continental Margin (eds Martinius AW, Ravn R., Howell JA, Steel RJ & Wonham JP): 19-58.
McKie, T., Audretsch, P., 2005. Depositional and structural controls on Triassic reservoir performance in the Heron Cluster, ETAP, Central North Sea. In: T. McKie, P. Audretsch (Eds.), Geological Society, London, Petroleum Geology Conference series. Geological Society of London, pp. 285-297.
Morad, S., 1998. Carbonate cementation in sandstones.
Morad, S., Al-Ramadan, K., Ketzer, J.M., De Ros, L., 2010. The impact of diagenesis on the heterogeneity of sandstone reservoirs: A review of the role of depositional facies and sequence stratigraphy. AAPG bulletin, 94(8): 1267-1309.
Morad, S., De Ros, L., Nystuen, J., Bergan, M., 1998. Carbonate diagenesis and porosity evolution in sheet‐flood sandstones: evidence from the Middle and Lower Lunde Members (Triassic) in the Snorre Field, Norwegian North Sea. Carbonate Cementation in Sandstones: Distribution Patterns and Geochemical Evolution: 53-85.
Naylor, H., Turner, P., Vaughan, D., Fallick, A., 1989. The Cherty Rock, Elgin: A petrographic and isotopic study of a Permo‐Triassic calcrete. Geological journal, 24(3): 205-221.
Nedkvitne, T., Karlsen, D.A., Bjørlykke, K., Larter, S.R., 1993. Relationship between reservoir diagenetic evolution and petroleum emplacement in the Ula Field, North Sea. Marine and Petroleum Geology, 10(3): 255-270.
Nguyen, B.T.T. et al., 2013. The role of fluid pressure and diagenetic cements for porosity preservation in Triassic fluvial reservoirs of the Central Graben, North Sea. AAPG Bulletin, 97(8): 1273-1302.
Paxton, S., Szabo, J., Ajdukiewicz, J., Klimentidis, R., 2002. Construction of an intergranular volume compaction curve for evaluating and predicting compaction and porosity loss in rigid-grain sandstone reservoirs. AAPG bulletin, 86(12): 2047-2067.

Purvis, K., Wright, V., 1991. Calcretes related to phreatophytic vegetation from the Middle Triassic Otter Sandstone of south west England. Sedimentology, 38(3): 539-551.
Ramm, M., Bjørlykke, K., 1994. Porosity/depth trends in reservoir sandstones: Assessing the quantitative effects of varying pore-pressure, temperature history and mineralogy, Norwegian Shelf data. Clay minerals, 29(4): 475-490.
Ramm, M., Forsberg, A.W., Jahren, J.S., 1997. Porosity--Depth Trends in Deeply Buried Upper Jurassic Reservoirs in the Norwegian Central Graben: An Example of Porosity Preservation Beneath the Normal Economic Basement by Grain-Coating Microquartz.
Salomons, W., Goudie, A., Mook, W., 1978. Isotopic composition of calcrete deposits from Europe, Africa and India. Earth Surface Processes, 3(1): 43-57.
Salomons, W., Mook, W., 1986. Isotope geochemistry of carbonates in the weathering zone. Handbook of environmental isotope geochemistry, 2: 239-269.
Schmidt, V., 1979. The role of secondary porosity in the course of sandstone diagenesis.
Sclater, J.G., Christie, P., 1980. Continental stretching; an explanation of the post-Mid-Cretaceous subsidence of the central North Sea basin. Journal of Geophysical Research, 85(B7): 3711-3739.
Smith, B.N., Epstein, S., 1971. Two categories of 13C/12C ratios for higher plants. Plant physiology, 47(3): 380-384.
Smith, R., Hodgson, N., Fulton, M., 1993. Salt control on Triassic reservoir distribution, UKCS central North Sea. In: R. Smith, N. Hodgson, M. Fulton (Eds.), Geological Society, London, Petroleum Geology Conference series. Geological Society of London, pp. 547-557.
Stewart, S., Clark, J., 1999. Impact of salt on the structure of the Central North Sea hydrocarbon fairways. In: S. Stewart, J. Clark (Eds.), Geological Society, London, Petroleum Geology Conference series. Geological Society of London, pp. 179-200.
Stricker, S., Jones, S.J., 2016. Enhanced porosity preservation by pore fluid overpressure and chlorite grain coatings in the Triassic Skagerrak, Central Graben, North Sea, UK. Geological Society, London, Special Publications, 435: SP435. 4.
Stricker, S., Jones, S.J., Grant, N.T., 2016a. Importance of vertical effective stress for reservoir quality in the Skagerrak Formation, Central Graben, North Sea. Marine and Petroleum Geology, 78: 895-909.
Stricker, S., Jones, S.J., Sathar, S., Bowen, L., Oxtoby, N., 2016b. Exceptional reservoir quality in HPHT reservoir settings: examples from the Skagerrak Formation of the Heron Cluster, UK, North Sea. Marine and Petroleum Geology, 77: 198-215.
Surdam, R.C., Boese, S.W., Crossey, L.J., 1984. The chemistry of secondary porosity: Part 2. Aspects of porosity modification.
Taylor, T.R., 1990. The influence of calcite dissolution on reservoir porosity in Miocene sandstones, Picaroon Field, offshore Texas Gulf Coast. Journal of Sedimentary Research, 60(3).
Taylor, T.R. et al., 2010. Sandstone diagenesis and reservoir quality prediction: Models, myths, and reality. AAPG Bulletin, 94(8): 1093-1132.
Taylor, T.R., Kittridge, M.G., Winefield, P., Bryndzia, L.T., Bonnell, L.M., 2015. Reservoir quality and rock properties modeling–Triassic and Jurassic sandstones, greater Shearwater area, UK Central North Sea. Marine and Petroleum Geology, 65: 1-21.
Vagle, G.B., Hurst, A., Dypvik, H., 1994. Origin of quartz cements in some sandstones from the Jurassic of the Inner Moray Firth (UK). Sedimentology, 41(2): 363-377.
Walderhaug, O., 1994. Precipitation rates for quartz cement in sandstones determined by fluid-inclusion microthermometry and temperature-history modeling. Journal of Sedimentary Research, 64(2).
Walderhaug, O., 1996. Kinetic modeling of quartz cementation and porosity loss in deeply buried sandstone reservoirs. AAPG bulletin, 80(5): 731-745.

Wang, J. et al., 2016. Pore fluid evolution, distribution and water-rock interactions of carbonate cements in red-bed sandstone reservoirs in the Dongying Depression, China. Marine and Petroleum Geology, 72: 279-294.

Xiong, D., Azmy, K., Blamey, N.J., 2016. Diagenesis and origin of calcite cement in the Flemish Pass Basin sandstone reservoir (Upper Jurassic): Implications for porosity development. Marine and Petroleum Geology, 70: 93-118.

Figures

Figure 1 Location map of the central North Sea showing wells and fields used in this study. The UK continental shelf (UKCS) and the Norway continental shelf (NOCS) boundaries are shown for reference.

Figure 2 General stratigraphy for the Triassic Skagerrak Formation of the study area, which is modified from Goldsmith et al. (2003) and Halland et al. (2014).

Figure 3 Geoseismic section of Central Graben. Inset map indicates line of section (modified from McKie, 2014).

Figure 4 Classification of Skagerrak Formation sandstones from the Norwegian wells used in this study based on Folk's classification (Folk, 1974) (Q: quartz, F: feldspar, R: rock fragment).

Figure 5 Grain size distribution for the Skagerrak Formation sandstones from specifically Cod, Ula and Gaupe fields.

Figure 6 Porosity distribution for the Skagerrak Formation sandstones from specifically Cod, Ula and Gaupe fields.

Figure 7 A) and B) Distribution of pore size for the Cod, Ula and Gaupe fields. C) and D) Distribution of pore area for the corresponding pore size. For data used from individual wells see the supplementary material.

Figure 8 A) Plot of compactional porosity loss (COPL) and cementational porosity loss (CEPL); B) Plot of intergranular volume and matrix. Data from all wells used in this study (see the supplementary material for data).

Figure 9 Petrography of quartz cementation and clay mineralogy. A) Quartz overgrowths are found in close association with ferroan dolomite (FD) in cross-polarized light (XPL), well 7/11-7R 4561.64

m; B) Euhedral quartz crystals occur as discontinuous quartz overgrowths and prismatic outgrowths on the top of chlorite coated grains in scanning electronic microscope (SEM), well 6/3-1 3104 m; C) SEM view showing occurrence of abundant microquartz, well 2/8-12 2541.13 m. Note that the crystallographic orientations of microquartz tend to be subparallel to the host grain surface, which is same as French and Worden (2013); D) SEM image of chlorite clay occurring as small plates and grain coats, well 7/12-6 3586 m; E) SEM image of illite occuring as pore bridging fibres that coexist with chlorite

coatings, well 6/3-1 3036.7 m; F) SEM image of smectite grain coatings which commonly occur throughout much of the Skagerrak Formation sandstones, well 7/7-2 3344 m.

Figure 10 A) Core photograph showing the occurrence of calcretes from well 6/3-1; B) Occurrence of large lithic fragments of calcrete as identified in thin section from channel base sandstone intervals. Location of thin section identified by arrow in (A), well 6/3-1 3089.45 m; C) Plain polarized light (PPL) of lithic calcrete fragment and associated carbonate cementation. Field of view is from black rectangle indicated in image (B). D) and E) showing poikilitic calcite and ankerite/ferroan dolomite (Ank/FD). Replacement of grain by carbonate cements can be found in both images, well 6/3-1 3035.05 m and well 7/11-7R 4582.06 m, respectively; F) SEM image of euhedral quartz and chlorite clays which predates poikilitic Ank/FD, well 6/3-1 3037 m; G) - I) showing sporadic euhedral and aggregated ankerite and/or ferroan dolomite, well 6/3-1 3110.00 m, well 7/7-2 3338 m and well 7/11-8 3742.1m, respectively.

Figure 11 Elemental mapping showing distribution of calcite for Ula (well 7/12-6) field and well 2/5-10. A) and B) Elemental mapping showing distribution of calcite cement (yellow colour). The content of calcite cement in well 7/12-6 at depth 3526.68 m is 19.81% (A) and markedly differs from well 2/5-10 at depth 4581 m

where it is 0.37% (B).

Figure 12 Carbon and Oxygen isotope data for calcite cement. The carbon and oxygen isotope data for calcite cement in this study show a narrow range of $\delta^{18}O$ values but a wide range of $\delta^{13}C$ values. The data are similar with previous carbonate cement analysis of Triassic sandstones (Bath et al. 1987; Knox et al. 1984; Morad et al. 1998; Naylor et al. 1989; Purvis and Wright, 1991; Saigal & Bjørlykke, 1987) (see text for details).

Figure 13 A) and B) K-feldspar dissolution from well 7/7-2 at 3344 m; C) Macropore from K-feldspar dissolution with associated euhedral ankerite/ferroan dolomite from well 7/11-7R at 4609.19 m; D) Framework grains with embayment shaped rims probably indicating early carbonate replacement and subsequent dissolution from well 6/3-1 at 3103.65 m.

Figure 14 Paragenetic sequence of Skagerrak Formation. The burial history curve is from Stricker et al. (2016a).

Figure 15 Fluid inclusion analysis of carbonate and quartz cements (from well 7/12-7 and well 7/12-6).

Figure 16 Porosity-depth plot for the Skagerrak Formation channel sandstone reservoirs from the UK section (Heron, Skua, Jade and Judy fields; Stricker et al., 2016a) and the Norwegian section (Cod, Ula and Gaupe fields), with exponential and linear trend lines in the North Sea (Scalter and Christie, 1980; Ramn and Bjørlykke, 1994).

Figure 17 Porosity versus carbonate cement. The diagram shows a positive relationship between porosity and carbonate cements at low carbonate cements content (< ~ 9%), whereas porosity decreases dramatically with carbonate cements increasing at high carbonate cements content (> ~ 9%).

Figure 18 A) Distribution of intergranular size for fine-grained

sandstones; B) Distribution of intergranular size for medium-grained sandstones; C) Cemented medium-grained sandstones, well 6/3-1 at depth of 3035.05 m; D) Uncemented medium-grained sandstones, well 6/3-1 at depth of 3069.4 m; E) Tight medium-grained sandstones, well 7/11-7R at depth of 4561.64 m (see text for details).

Figure 19 Relationship between precipitation temperature and oxygen isotope ratio of calcite cement. The diagram indicates that the precipitation temperature of calcite cement is around 11 °C (see text for details).

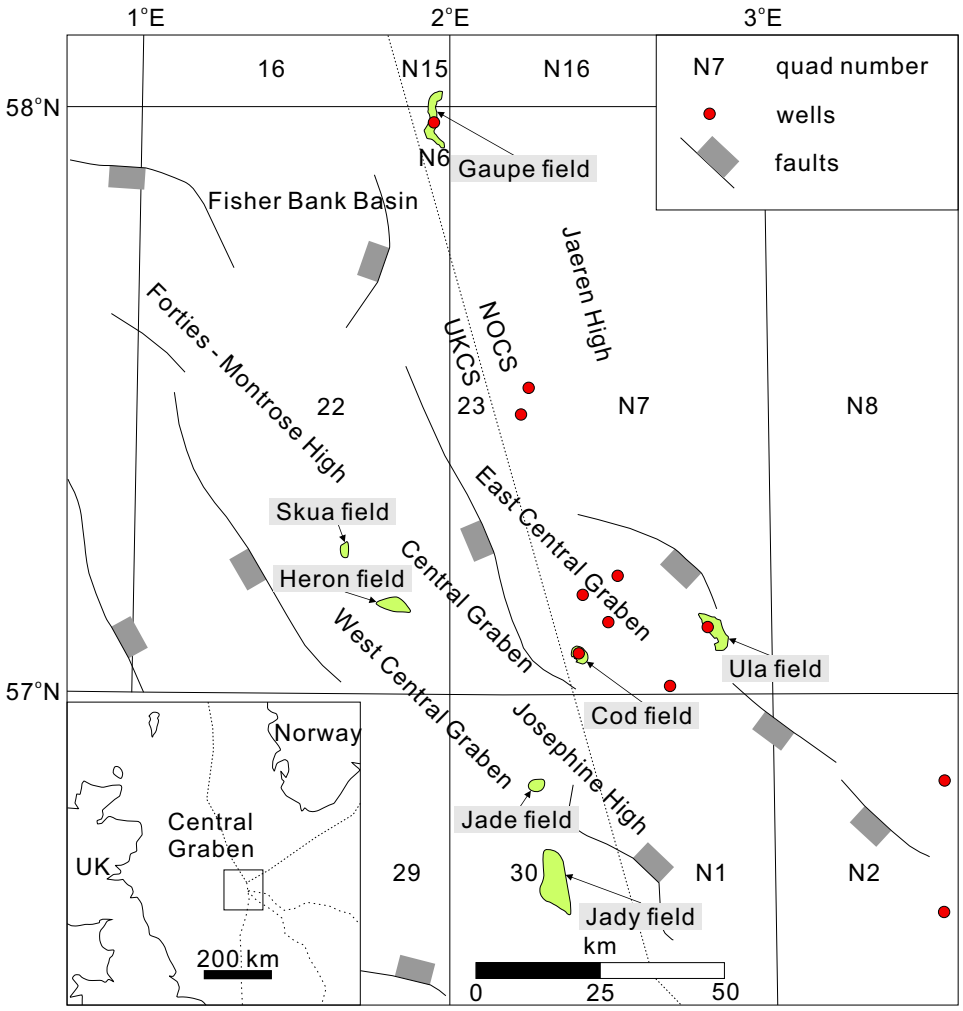
1°E
2°E
3°E
58°N
57°N
16
N15
N16
N7
quad number
wells
faults
N6
Gaupe field
Fisher Bank Basin
Jaeren High
NOCS
UKCS
Forties - Montrose High
22
23
N7
N8
East Central Graben
Skua field
Heron field
Central Graben
West Central Graben
Ula field
Cod field
Josephine High
Jade field
Jady field
29
30
N1
N2
Norway
Central
Graben
UK
200 km
km
0
25
50

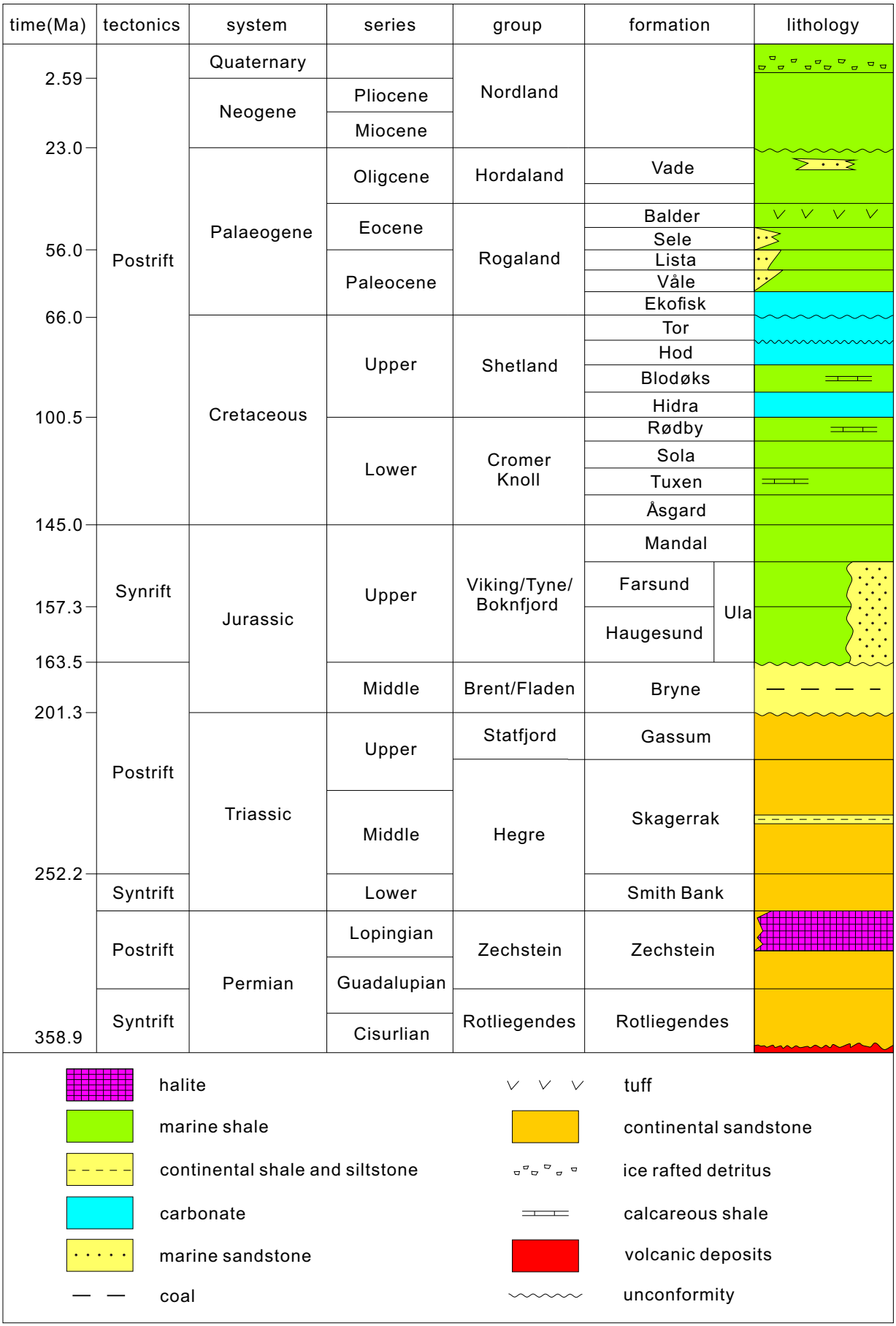
time(Ma)
tectonics
system
series
group
formation
lithology
2.59
23.0
56.0
66.0
100.5
145.0
157.3
163.5
201.3
252.2
358.9
Postrift
Synrift
Postrift
Syntrift
Postrift
Syntrift
Quaternary
Neogene
Palaeogene
Cretaceous
Jurassic
Triassic
Permian
Pliocene
Miocene
Oligcene
Eocene
Paleocene
Upper
Lower
Upper
Middle
Upper
Middle
Lower
Lopingian
Guadalupian
Cisurlian
Nordland
Hordaland
Rogaland
Shetland
Cromer Knoll
Viking/Tyne/ Boknfjord
Brent/Fladen
Statfjord
Hegre
Zechstein
Rotliegendes
Vade
Balder
Sele
Lista
Våle
Ekofisk
Tor
Hod
Blodøks
Hidra
Rødby
Sola
Tuxen
Åsgard
Mandal
Farsund
Haugesunde
Ula
Bryne
Gassum
Skagerrak
Smith Bank
Zechstein
Rotliegendes
halite
marine shale
continental shale and siltstone
carbonate
marine sandstone
coal
tuff
continental sandstone
ice rafted detritus
calcareous shale
volcanic deposits
unconformity

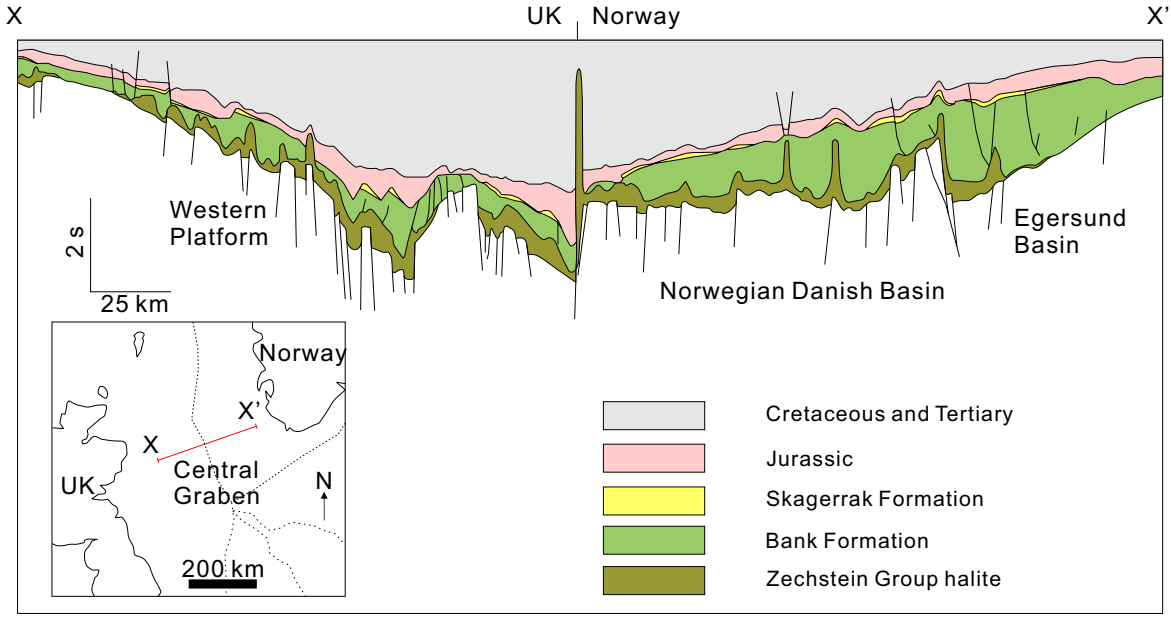
X
UK
Norway
X'
Western
Platform
2 s
25 km
Egersund
Basin
Norwegian Danish Basin
Norway
X'
X
Central
Graben
UK
N
200 km
Cretaceous and Tertiary
Jurassic
Skagerrak Formation
Bank Formation
Zechstein Group halite

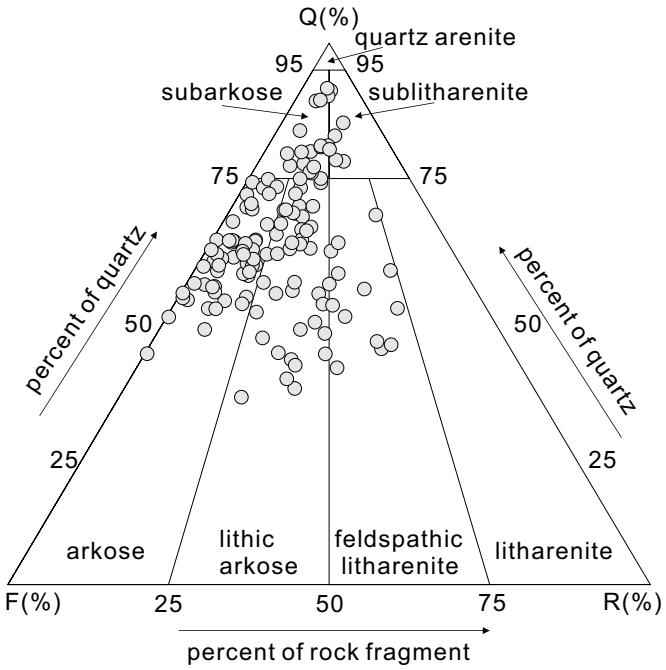
Q(%)
quartz arenite
95
95
subarkose
sublitharenite
75
75
percent of quartz
50
50
percent of quartz
25
25
arkose
lithic
arkose
feldspathic
litharenite
litharenite
F(%)
25
50
75
R(%)
percent of rock fragment

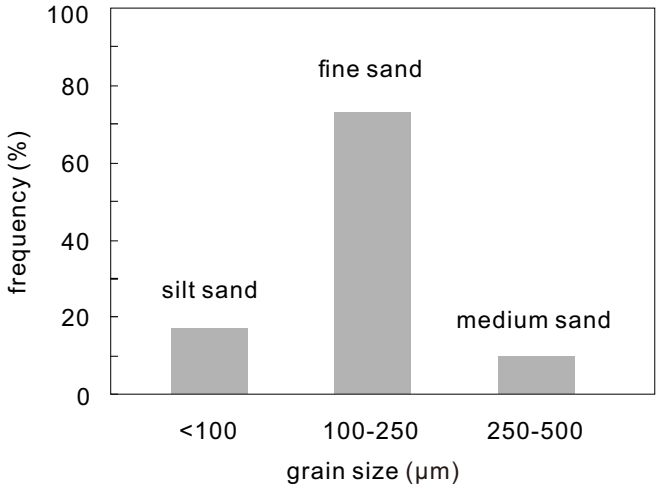
100
80
60
40
20
0
frequency (%)
silt sand
fine sand
medium sand
<100
100-250
250-500
grain size (μm)

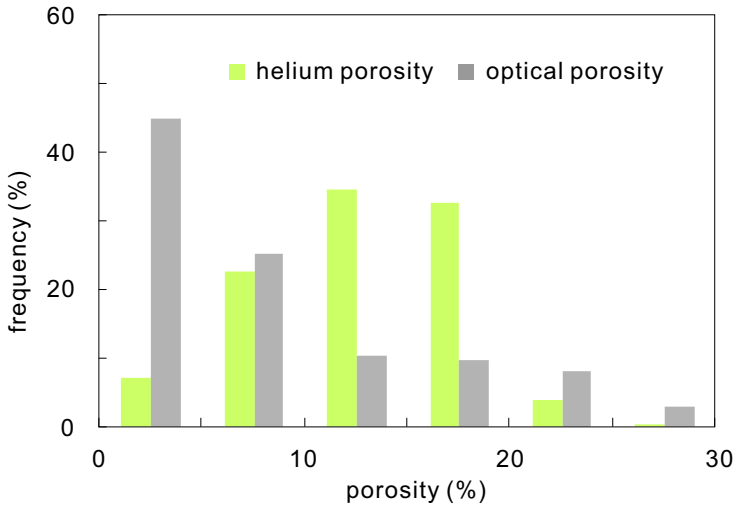
60
40
20
0
frequency (%)
helium porosity
optical porosity
0
10
20
30
porosity (%)

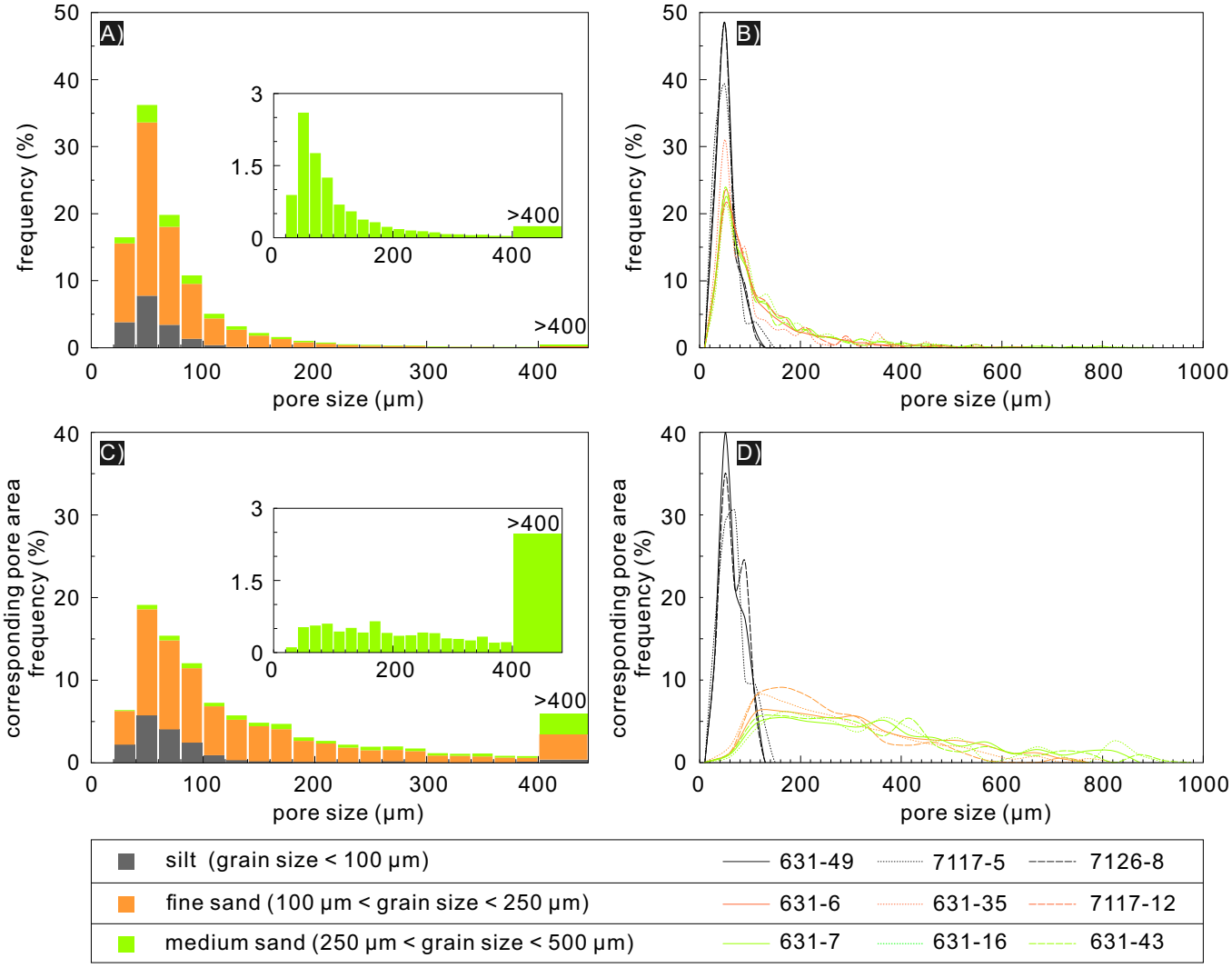
A)
B)
C)
D)
frequency (%)
corresponding pore area frequency (%)
pore size (µm)
>400
silt (grain size < 100 µm)
fine sand (100 µm < grain size < 250 µm)
medium sand (250 µm < grain size < 500 µm)
631-49
7117-5
7126-8
631-6
631-35
7117-12
631-7
631-16
631-43

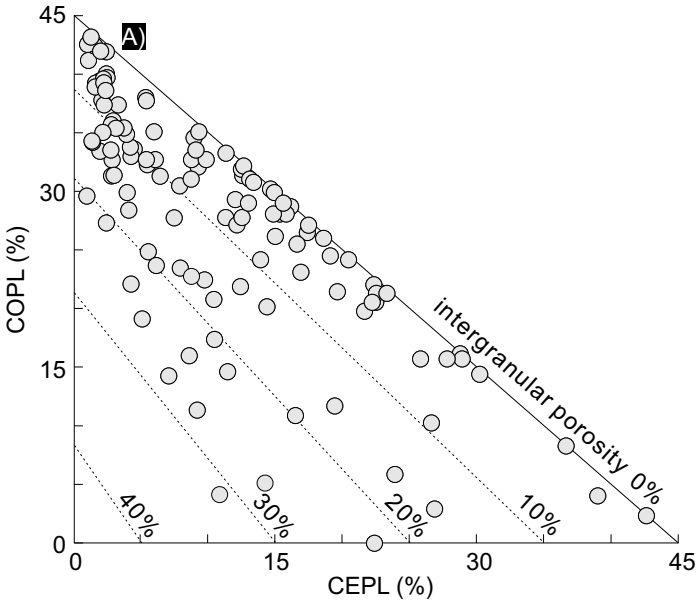
A)
COPL (%)
CEPL (%)
intergranular porosity 0%
10%
20%
30%
40%
0
15
30
45

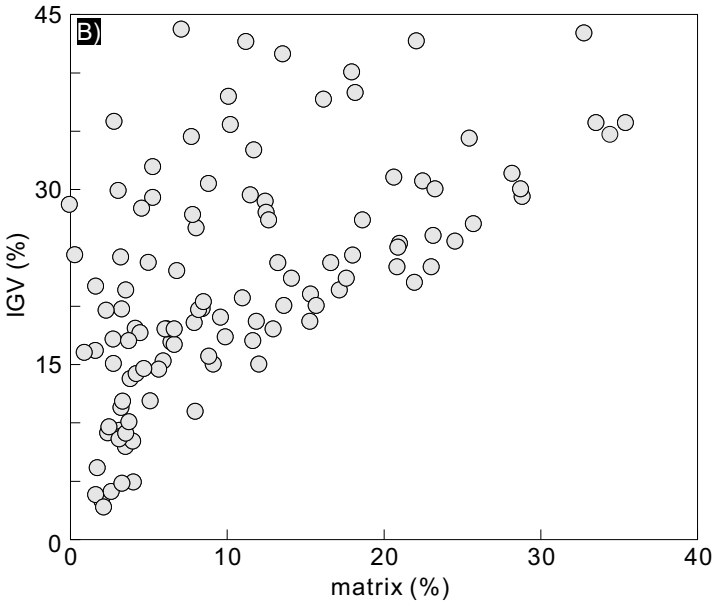
B)
IGV (%)
matrix (%)
0
10
20
30
40
15
30
45

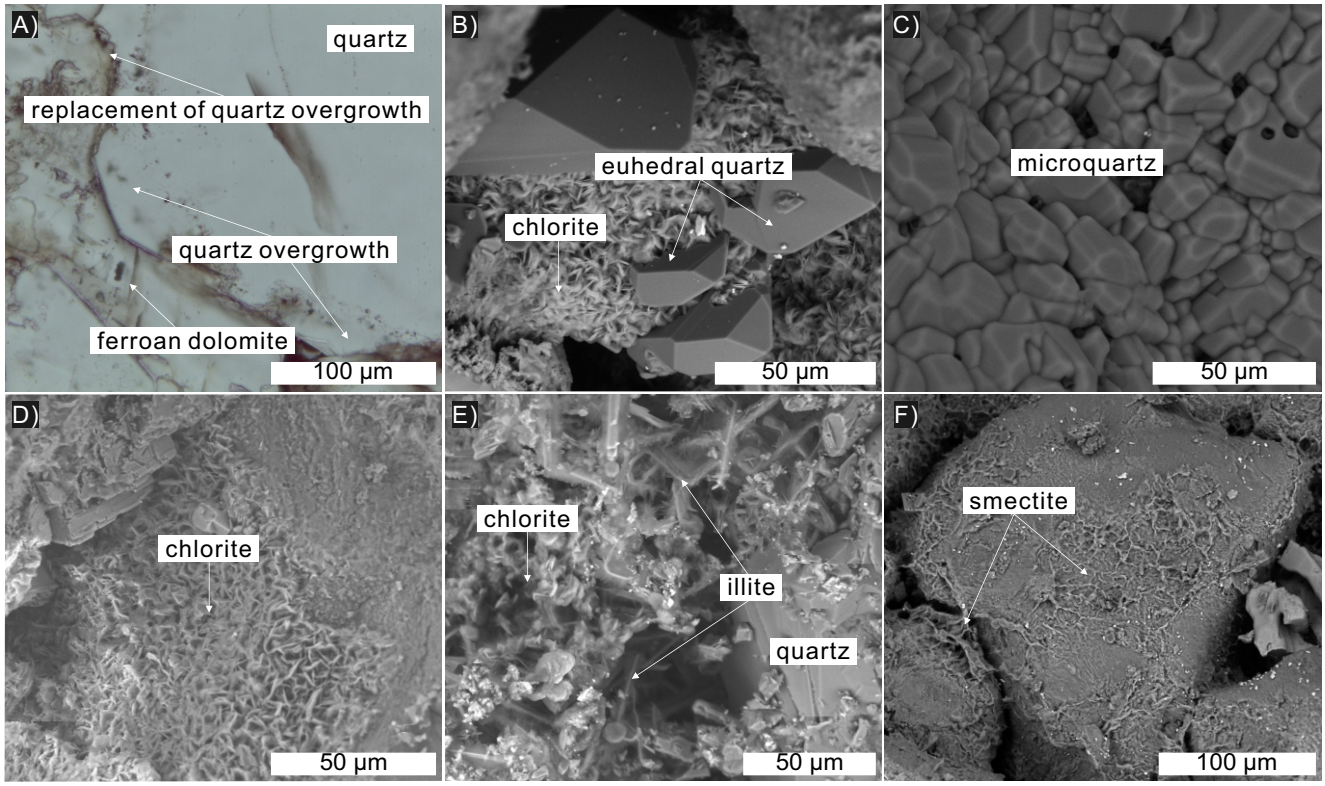
A)
quartz
replacement of quartz overgrowth
quartz overgrowth
ferroan dolomite
100 µm
B)
euhedral quartz
chlorite
50 µm
C)
microquartz
50 µm
D)
chlorite
50 µm
E)
chlorite
illite
quartz
50 µm
F)
smectite
100 µm

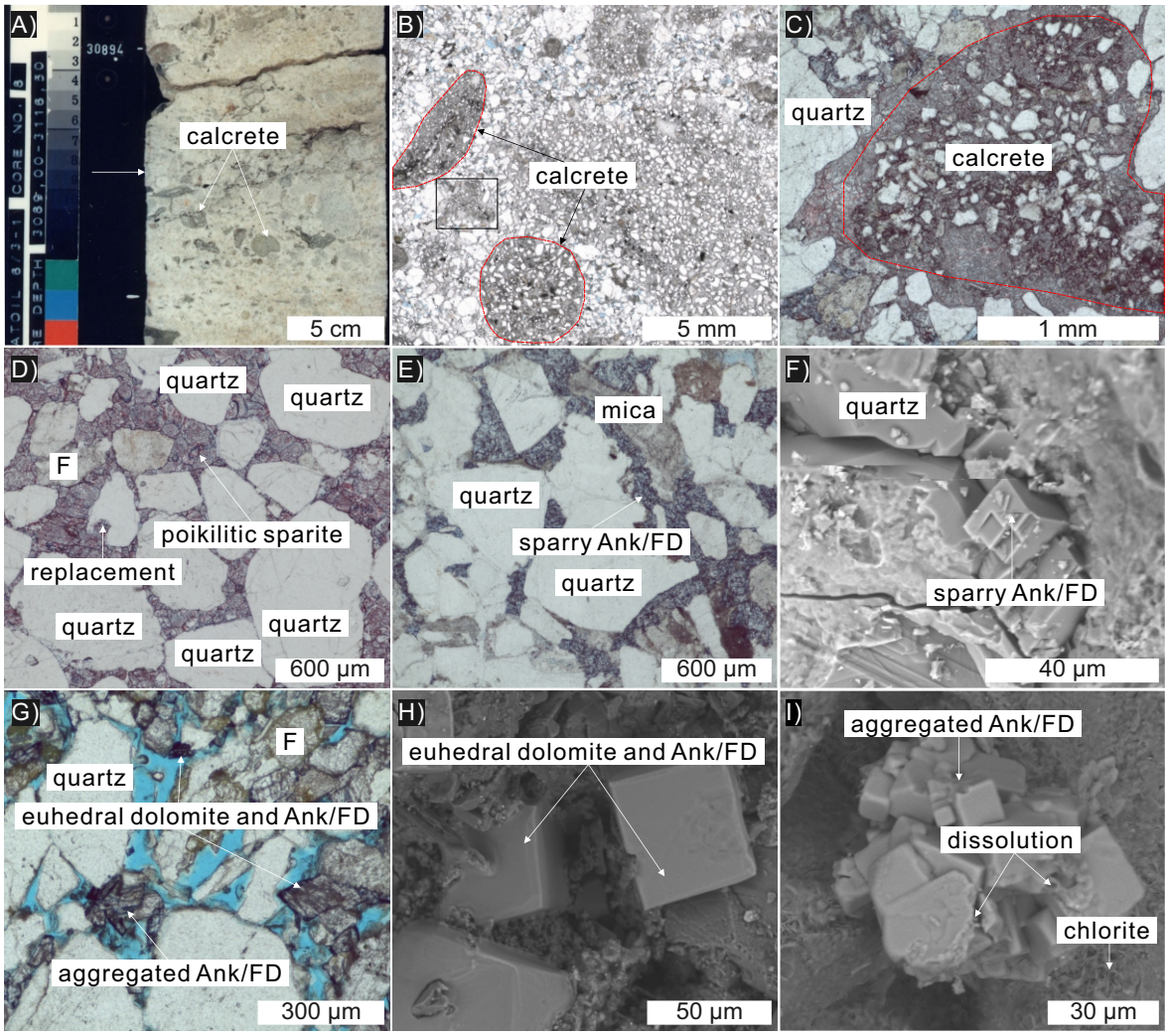
A)
calcrete
5 cm
B)
calcrete
5 mm
C)
quartz
calcrete
1 mm
D)
quartz
quartz
F
poikilitic sparite
replacement
quartz
quartz
quartz
600 µm
E)
mica
quartz
sparry Ank/FD
quartz
600 µm
F)
quartz
sparry Ank/FD
40 µm
G)
F
quartz
euhedral dolomite and Ank/FD
aggregated Ank/FD
300 µm
H)
euhedral dolomite and Ank/FD
50 µm
I)
aggregated Ank/FD
dissolution
chlorite
30 µm

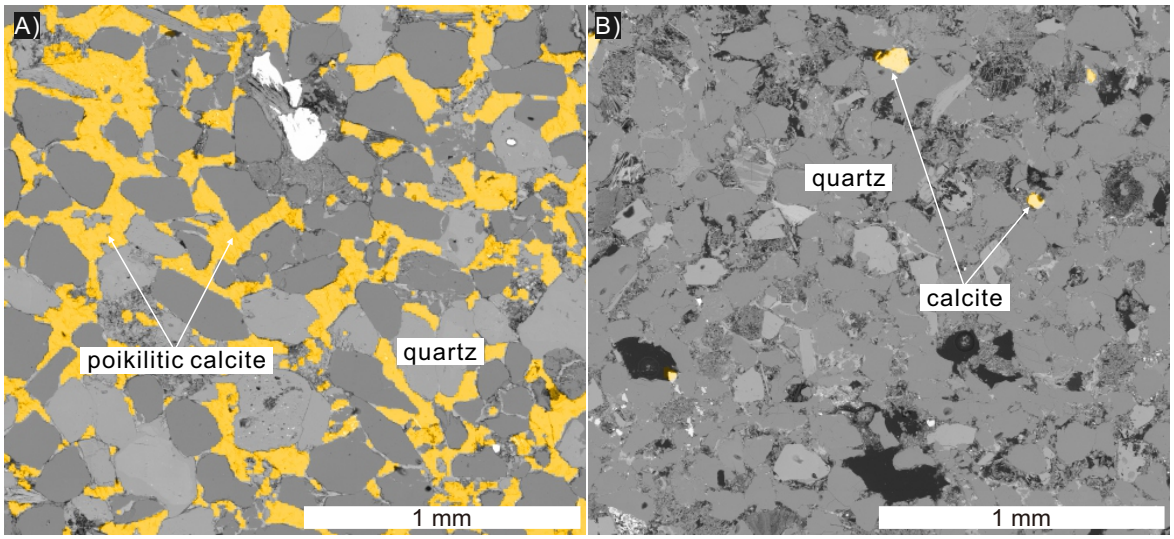
A)
poikilitic calcite
quartz
1 mm
B)
quartz
calcite
1 mm

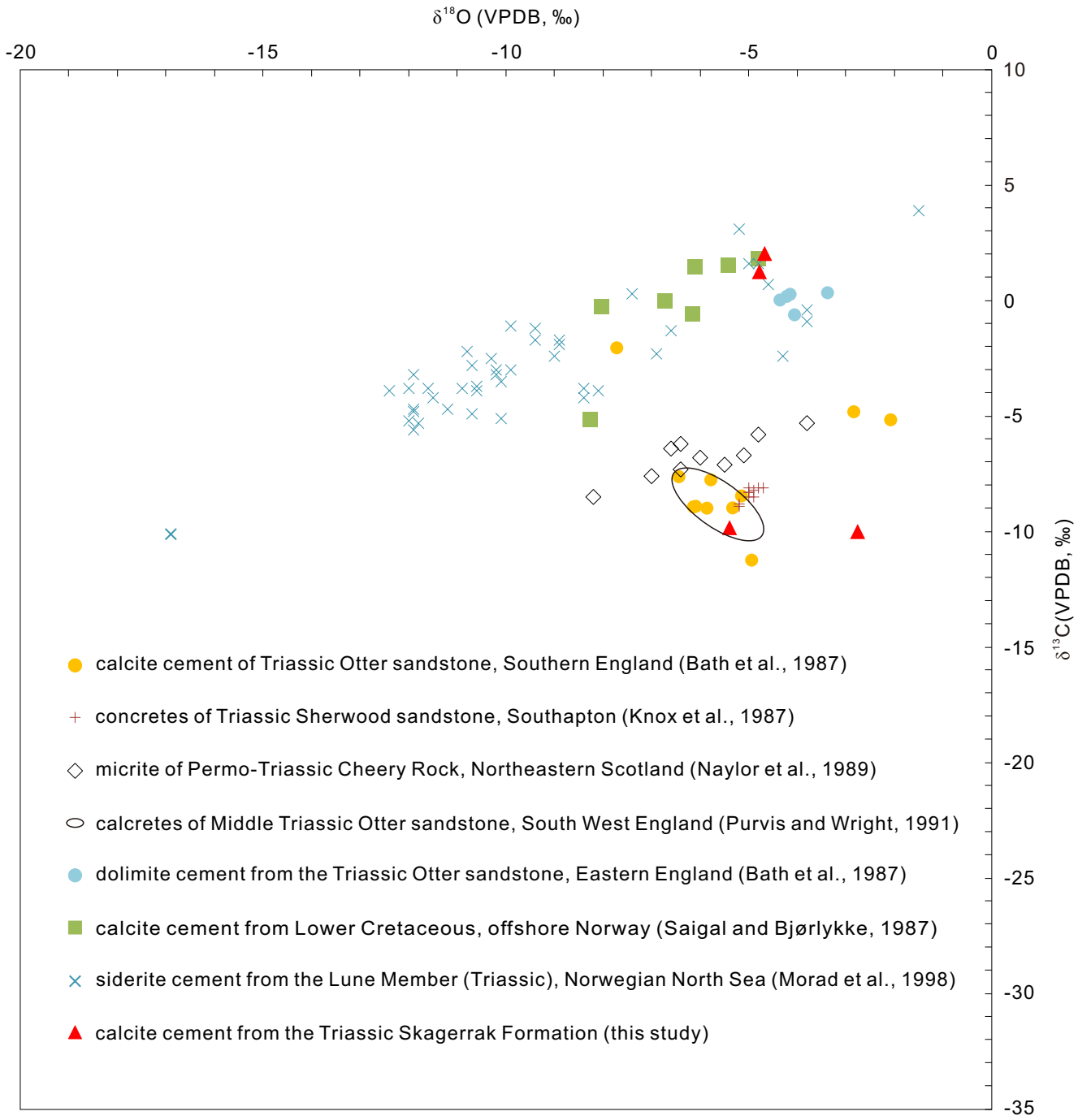
δ18O (VPDB, ‰)
-20
-15
-10
-5
0
10
5
0
-5
-10
-15
-20
-25
-30
-35
δ13C(VPDB, ‰)
calcite cement of Triassic Otter sandstone, Southern England (Bath et al., 1987)
concretes of Triassic Sherwood sandstone, Southapton (Knox et al., 1987)
micrite of Permo-Triassic Cheery Rock, Northeastern Scotland (Naylor et al., 1989)
calcretes of Middle Triassic Otter sandstone, South West England (Purvis and Wright, 1991)
dolimite cement from the Triassic Otter sandstone, Eastern England (Bath et al., 1987)
calcite cement from Lower Cretaceous, offshore Norway (Saigal and Bjørlykke, 1987)
siderite cement from the Lune Member (Triassic), Norwegian North Sea (Morad et al., 1998)
calcite cement from the Triassic Skagerrak Formation (this study)

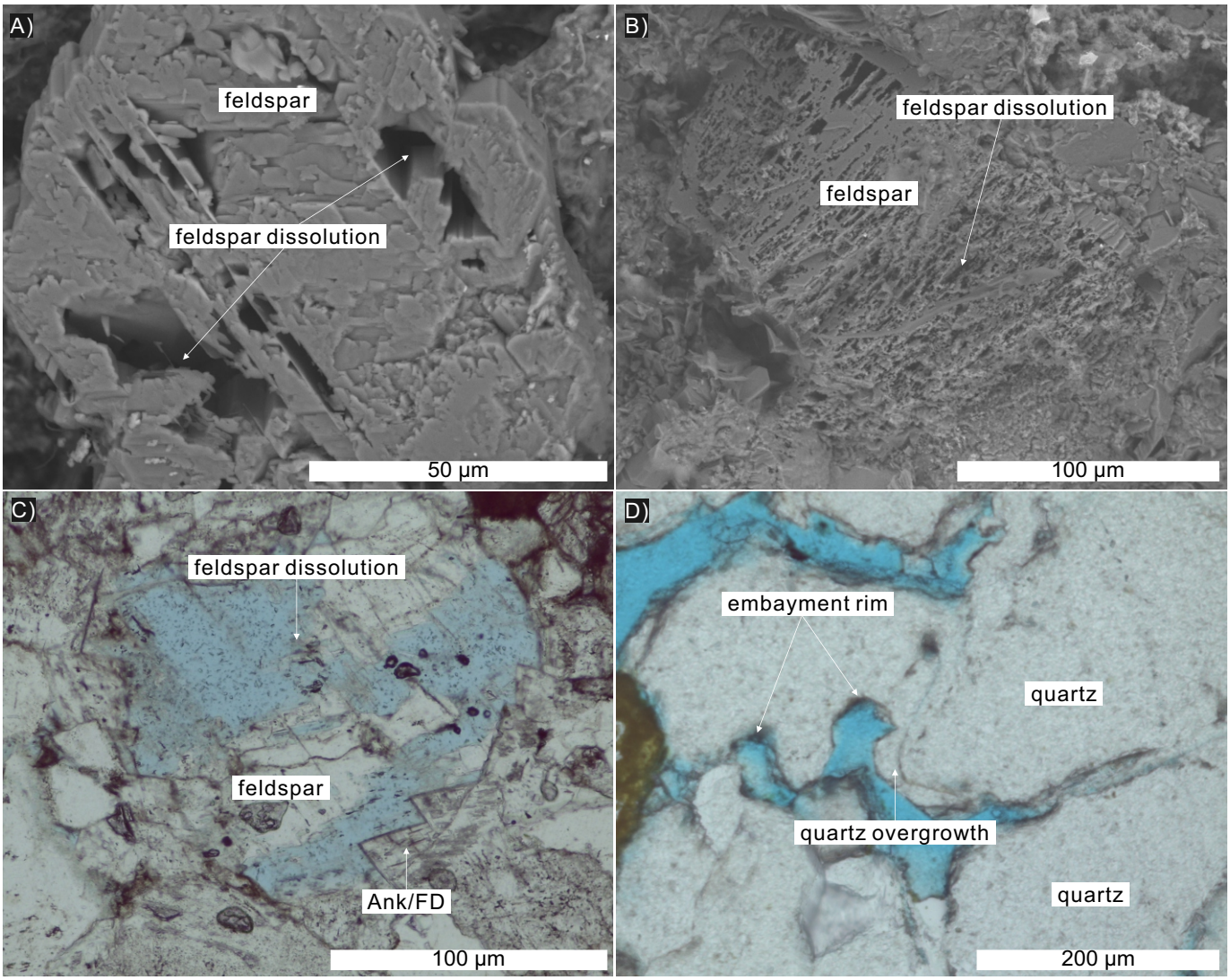
A)
feldspar
feldspar dissolution
50 µm
B)
feldspar dissolution
feldspar
100 µm
C)
feldspar dissolution
feldspar
Ank/FD
100 µm
D)
embayment rim
quartz
quartz overgrowth
quartz
200 µm

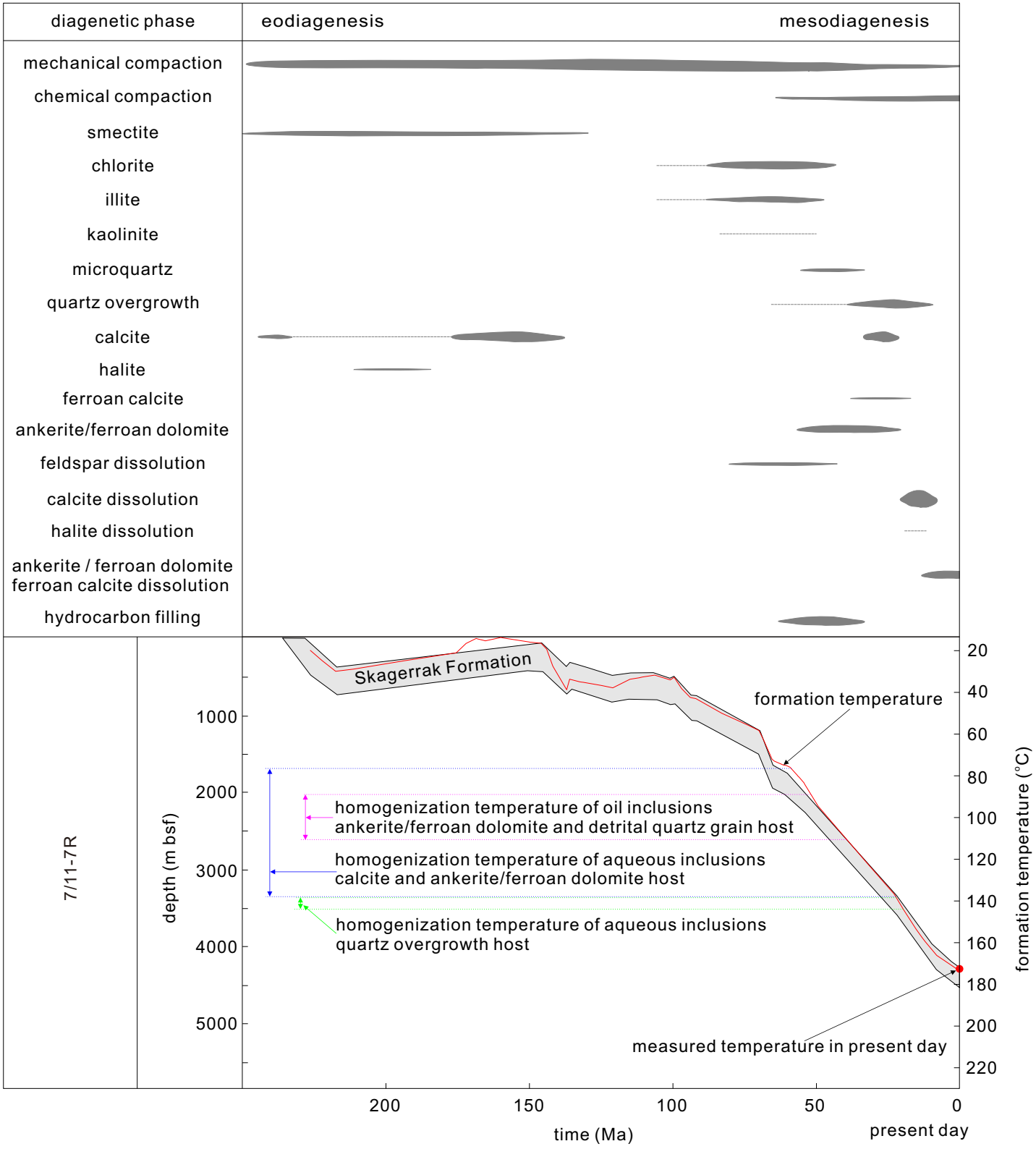
diagenetic phase
eodiagenesis
mesodiagenesis
mechanical compaction
chemical compaction
smectite
chlorite
illite
kaolinite
microquartz
quartz overgrowth
calcite
halite
ferroan calcite
ankerite/ferroan dolomite
feldspar dissolution
calcite dissolution
halite dissolution
ankerite / ferroan dolomite
ferroan calcite dissolution
hydrocarbon filling
7/11-7R
depth (m bsf)
1000
2000
3000
4000
5000
Skagerrak Formation
formation temperature
homogenization temperature of oil inclusions
ankerite/ferroan dolomite and detrital quartz grain host
homogenization temperature of aqueous inclusions
calcite and ankerite/ferroan dolomite host
homogenization temperature of aqueous inclusions
quartz overgrowth host
measured temperature in present day
20
40
60
80
100
120
140
160
180
200
220
formation temperature (°C)
200
150
100
50
0
time (Ma)
present day

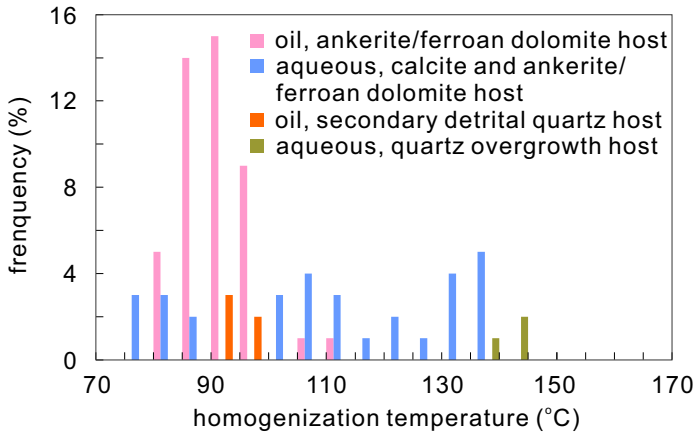
16
12
8
4
0
frenquency (%)
70
90
110
130
150
170
homogenization temperature (°C)
oil, ankerite/ferroan dolomite host
aqueous, calcite and ankerite/ ferroan dolomite host
oil, secondary detrital quartz host
aqueous, quartz overgrowth host

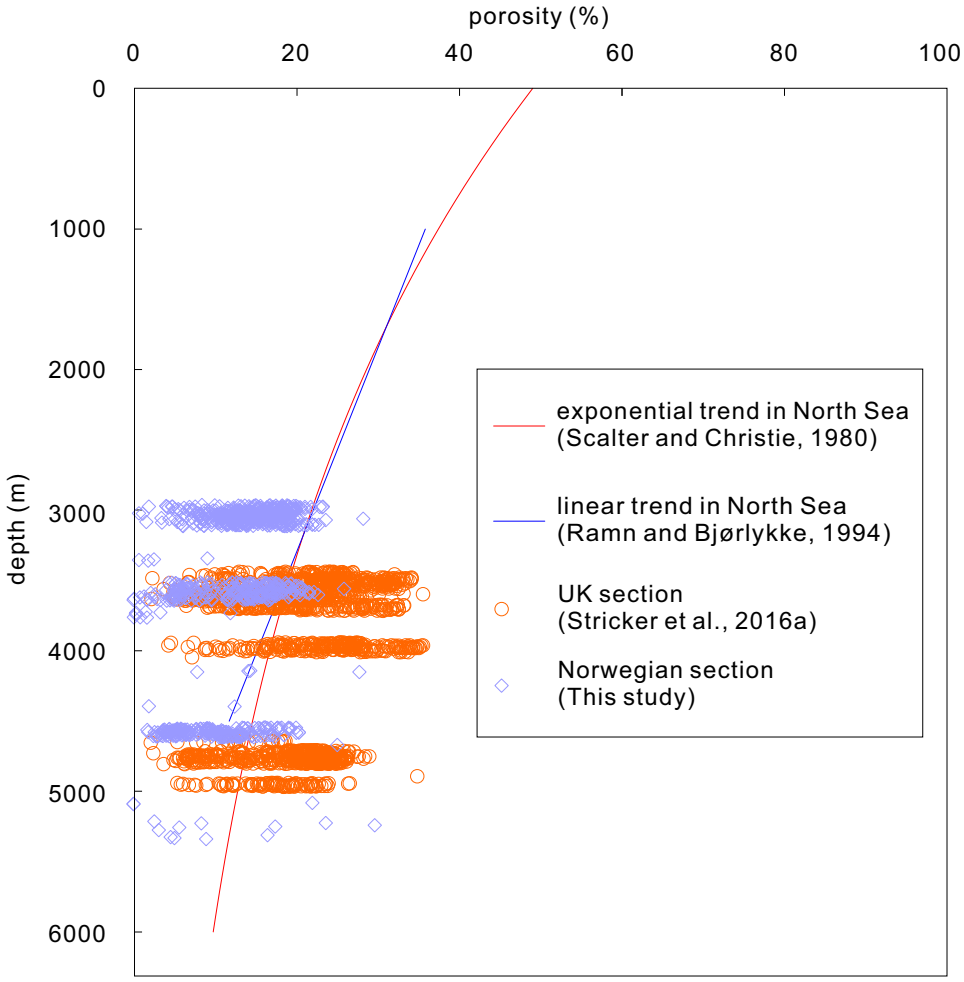
porosity (%)
0
20
40
60
80
100
depth (m)
0
1000
2000
3000
4000
5000
6000
exponential trend in North Sea
(Scalter and Christie, 1980)
linear trend in North Sea
(Ramn and Bjørlykke, 1994)
UK section
(Stricker et al., 2016a)
Norwegian section
(This study)

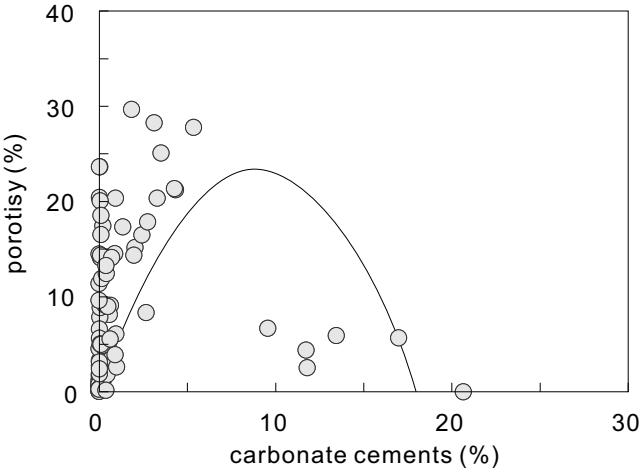
40
30
20
10
0
porotisy (%)
0
10
20
30
carbonate cements (%)

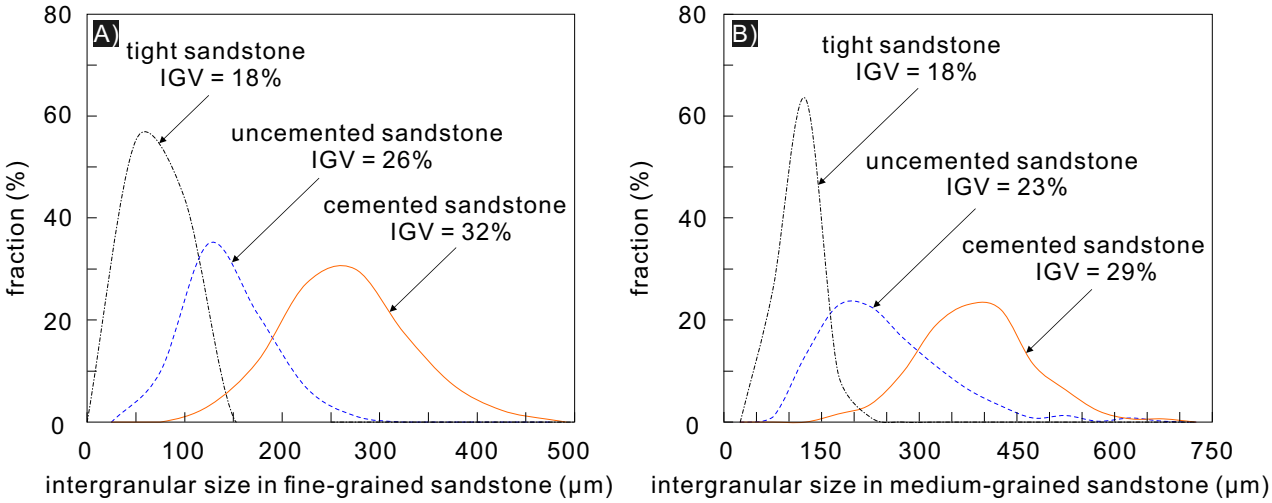
A)
tight sandstone
IGV = 18%
uncemented sandstone
IGV = 26%
cemented sandstone
IGV = 32%
fraction (%)
intergranular size in fine-grained sandstone (μm)
B)
tight sandstone
IGV = 18%
uncemented sandstone
IGV = 23%
cemented sandstone
IGV = 29%
fraction (%)
intergranular size in medium-grained sandstone (μm)

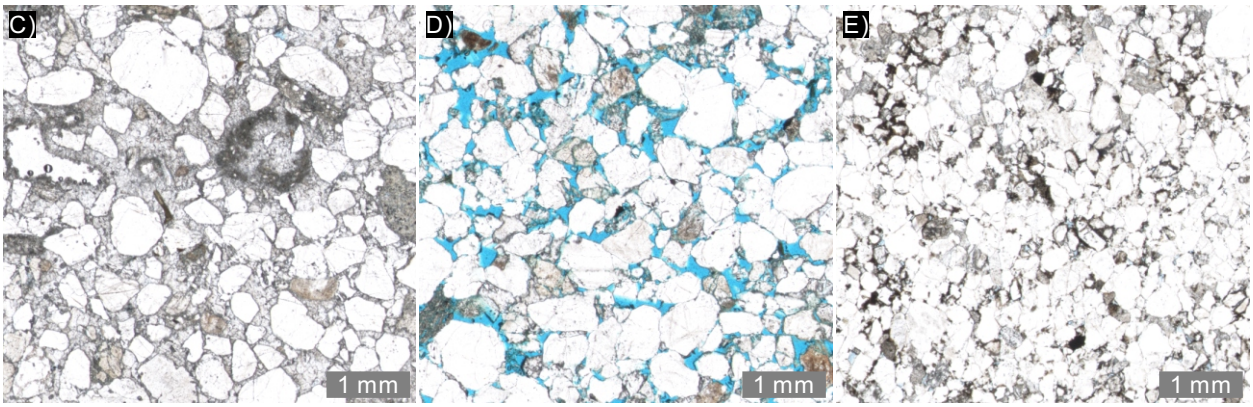
C)
1 mm
D)
1 mm
E)
1 mm

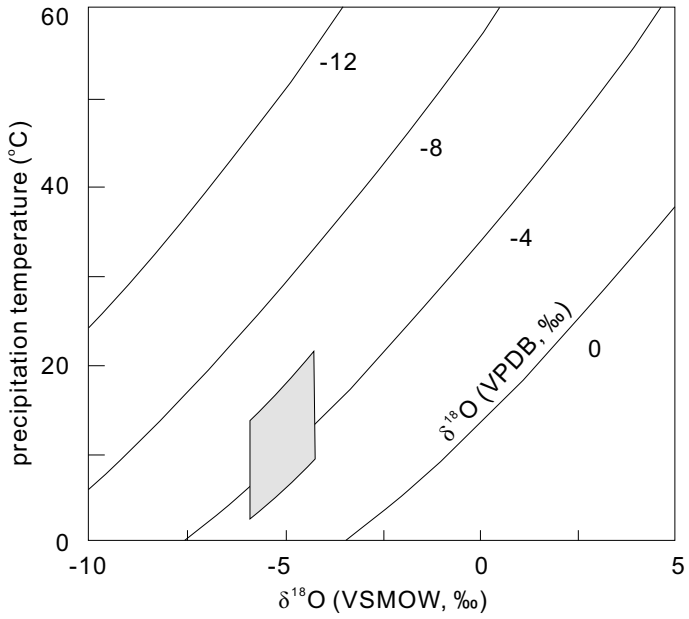
60
40
20
0
precipitation temperature (°C)
-12
-8
-4
0
δ18O (VPDB, ‰)
-10
-5
0
5
δ18O (VSMOW, ‰)